



INSTITUT DE FRANCE
Académie des sciences

Comptes Rendus

Géoscience

Sciences de la Planète

Didier Bertil, Nicolas Mercury, Cécile Doubre, Anne Lemoine
and Jérôme Van der Woerd

**The unexpected Mayotte 2018–2020 seismic sequence: a reappraisal of
the regional seismicity of the Comoros**


Volume 353, issue S1 (2021), p. 211-235

<<https://doi.org/10.5802/crgeos.79>>

Part of the Special Issue: Seismicity in France

Guest editors: Carole Petit (Université Côte d'Azur, CNRS, IRD, Observatoire de la Côte d'Azur), Stéphane Mazzotti (Univ. Montpellier & CNRS, France) and Frédéric Masson (Université de Strasbourg & CNRS, France)

© Académie des sciences, Paris and the authors, 2021.
Some rights reserved.

 This article is licensed under the
CREATIVE COMMONS ATTRIBUTION 4.0 INTERNATIONAL LICENSE.
<http://creativecommons.org/licenses/by/4.0/>



*Les Comptes Rendus. Géoscience — Sciences de la Planète sont membres du
Centre Mersenne pour l'édition scientifique ouverte*
www.centre-mersenne.org



Seismicity in France / *Sismicité en France*

The unexpected Mayotte 2018–2020 seismic sequence: a reappraisal of the regional seismicity of the Comoros

Didier Bertil^{® *},^a, Nicolas Mercury^{a, b}, Cécile Doubre^{® b}, Anne Lemoine^{® a}
and Jérôme Van der Woerd^{® b}

^a BRGM, Department of Risks and Prevention, 3 av. Claude-Guillemin - BP 36009,
45060 Orléans Cedex 2, France

^b Institut Terre Environnement de Strasbourg, UMR 7063 Université de Strasbourg,
CNRS, 5 rue René Descartes, 67084 Strasbourg Cedex, France

E-mails: d.bertil@brgm.fr (D. Bertil), n.mercury@brgm.fr (N. Mercury),
cecile.doubre@unistra.fr (C. Doubre), a.lemoine@brgm.fr (A. Lemoine),
jerome.vanderwoerd@unistra.fr (J. Van der Woerd)

Abstract. The Mayotte seismic sequence that started on 10 May 2018, with a main shock of magnitude Mw 5.9 on May 15, followed by a major offshore volcanic activity, raises several questions of seismo-volcanic hazards in the Comoros region. The unexpected size and duration of the crisis is an opportunity to reassess the distribution and magnitude of the seismicity near Mayotte Island, but also regionally. We present a comprehensive seismicity catalogue of the region including the Mozambique Channel, the Mozambique coast and Madagascar, based partly on previously published data in the region and partly on unpublished data from local catalogues for the Comoros and Madagascar. Our catalogue extends from 1900 onward with a completeness of magnitude 5.5 until 1980s and decreasing only recently to 4.5 after 2010. It comprises the events of magnitude $M_{lv} \geq 3.5$ for the seismic sequence of Mayotte from May 2018 to October 2020 as the crisis is still ongoing. Present knowledge of the seismicity, largely partial in distribution and magnitude before 1980, makes the seismic sequence of 2018–2020 an exceptional and unprecedented seismo-volcanic event in the region. We discuss the distribution of seismicity in time and space within the context of the south eastward propagation of the East African rift system towards Madagascar.

Keywords. Seismicity, Seismo-volcanic hazard, Comoros, Mayotte, Mozambique Channel.

Available online 13th September 2021

1. Introduction

The occurrence of natural seismic events in unexpected places such as the intraplate domain challenges our understanding of both local and regional tectonics. The ongoing seismic sequence of

2018–2020 near Mayotte Island is no exception. While the volcanic islands of the Comoros archipelago are known for their moderate seismicity, the seismic event of 15 May 2018 of magnitude Mw 5.9 (Mayotte, France), the following long-lasting seismic sequence [Bertil et al., 2019, Lemoine et al., 2019, 2020a, Cesca et al., 2019, 2020, Saurel et al., 2019, 2021, Jacques et al., 2019] and the discovery of a

* Corresponding author.

new active offshore volcano east of Mayotte [Feuillet *et al.*, 2019a, 2021] led geoscientists and authorities to reassess the seismic, volcanic and tsunami hazard and related risks not only in Mayotte but also in the whole northern Mozambique Channel region [e.g., Lemoine *et al.*, 2020b]. The monitoring seismic networks are still poorly developed in the surrounding countries and remain limited due to the isolated nature of small oceanic islands, together with the sparseness or the lack of historical archives, significantly limiting our knowledge of past natural hazards and a more fundamental understanding of the geodynamic and volcano-tectonic context of the region.

The region under study, located southeast of Africa, is characterized by moderate and scattered seismicity mainly distributed in the Mozambique Channel, in Madagascar, along the Comoros archipelago and at the southern tip of the East African Rift System (EARS; Figure 1). The origin and nature of the deformation affecting the region remain poorly constrained over the long term as well as the short term. Several main geodynamic events have interplayed in the region, such as the formation of the Mozambique and Somali Basins, with late Jurassic oceanic spreading, and the slow opening of the EARS fragmenting the southeast of the African continent during the Tertiary. The volcanism occurring at distinct places of this wide region, and particularly along the Comoros archipelago, is seen as the result of intraplate magmatism, whose origin is discussed in the frame of the well-known debate between an active ascent from the deep mantle and the role of lithospheric stresses [Morgan, 1972, Michon, 2016, and references therein]. Whereas the long-term tectonic plate motion models are regularly re-evaluated due to the increase in geophysical studies in the region [e.g. Horner-Johnson *et al.*, 2007, König and Jokat, 2010, Davis *et al.*, 2016], the short-term kinematic models are also regularly revised taking into account the ongoing development of the geodetic networks [Déprez *et al.*, 2013, Saria *et al.*, 2013, Stamps *et al.*, 2014, 2018, 2020]. However, the sparseness of GNSS stations mainly due to the large extent of oceans prevents the proper constraining of the contours, number and motion of the tectonic plates and their respective kinematics. The unexpected and exceptional recent Mayotte seismo-volcanic sequence has renewed the scientific interest in the north Mozambique Channel, and has

evidenced the necessary reappraisal of its seismic activity to better address the processes involved in the deformation of the region and better estimate the respective role of magmatism, tectonics and inheritance in the current deformation along the axis of the Comoros Archipelago.

2. Geodynamic context

The breakup of the Gondwana supercontinent in the Mesozoic led to the opening of the west Somali and Mozambique Basins [Davis *et al.*, 2016]. India and Madagascar drifted southeastward due to the extension across northeast–southwest oriented rifts separated by the Davie Ridge acting as a transform fault [Malod *et al.*, 1991]. The current location of Madagascar relative to Nubia is inherited since the end of rifting in the west Somali and Mozambique Basins in the lower Cretaceous (120 Ma), indicating limited subsequent deformation at the plate tectonic scale, especially during the Cretaceous–Tertiary with the separation of India from Madagascar as well as the southward propagation of the EARS. These latter events were accompanied by intense regional volcanism in the large volcanic provinces of the Deccan Traps and La Réunion hot spot (65 Ma) and in southern Tanzania since late Oligocene.

The EW-trending Comoros archipelago is located between the rifted oceanic crust of the west Somali basin in the north [Rabinowitz *et al.*, 1983, Coffin and Rabinowitz, 1987, Davis *et al.*, 2016] and the Comoros basin to the south, whose crustal nature remains unclear [Phethean *et al.*, 2016]. The archipelago may be impinging the continental margin of northern Madagascar, which is also suggested by the presence of rocks of continental origin outcropping in the volcanic islands of the Comoros [Flower and Strong, 1969]. However, the origin of such an alignment remains unclear and the nature of this feature in the tectonic context is debated. While the younging of the volcanism from east (~20 to 10 Ma in Mayotte) to west (9 or 1 Ma to present in Grande Comore) [Pelletier *et al.*, 2014, Michon, 2016] has been suggested to reflect the impingement of a hot spot into the lithosphere, it is neither supported by the motion of the Somalia plate, nor by the new volcanic rock dating across the archipelago [Michon, 2016, Bachèlery *et al.*, 2016, Leroux *et al.*, 2020] and the recent volcanic activity east of Mayotte [Feuillet *et al.*, 2021].

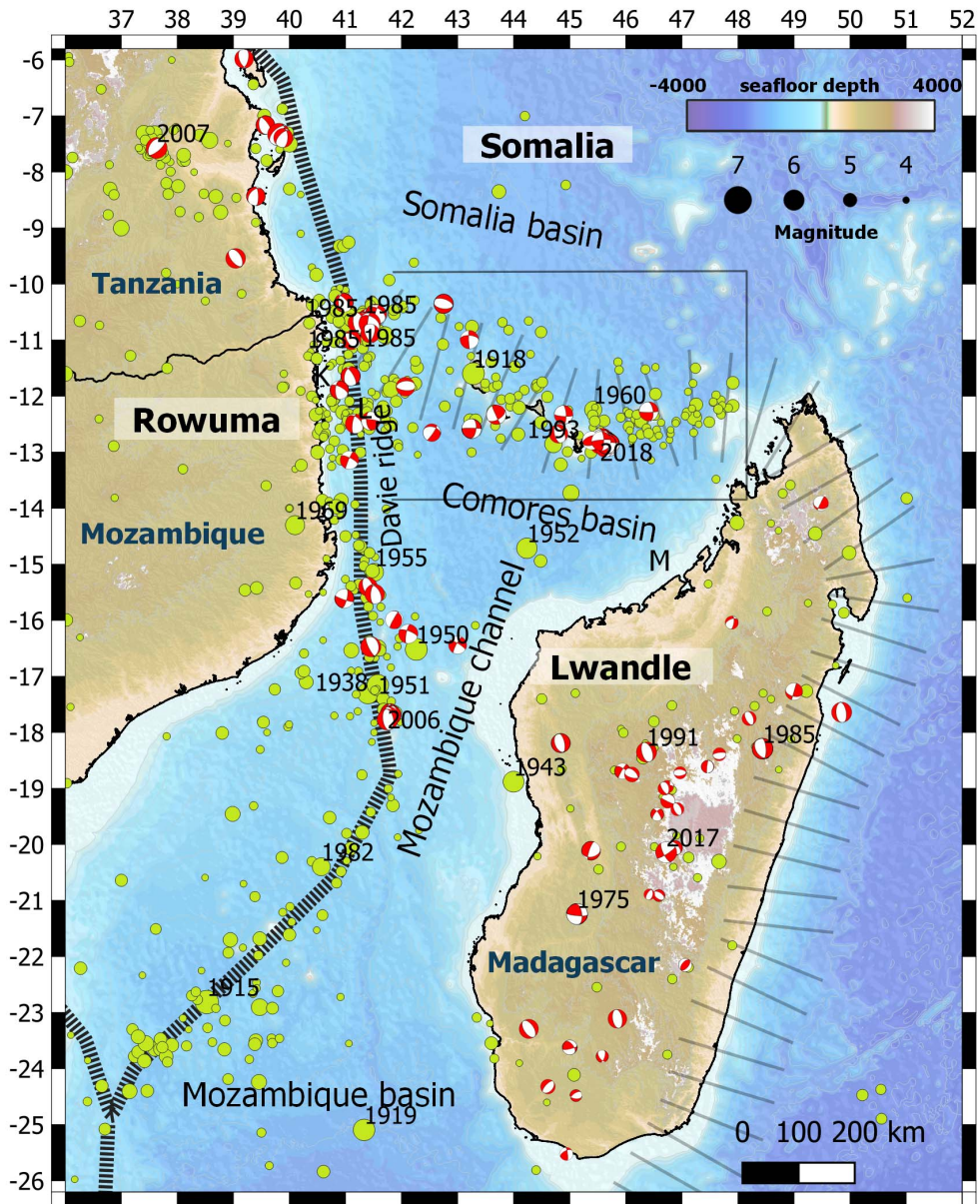


Figure 1. Seismicity of magnitude ≥ 4 from 1900 to 1/10/2020 across the Mozambique Channel and its surrounding areas. Hatched bands represent the plate boundaries of Rovuma and Lwandle proposed by several authors [e.g., Kusky *et al.*, 2007, Stamps *et al.*, 2018]. Widely hatched bands represent supposed but poorly constrained Lwandle boundaries [from Lemoine *et al.*, 2020a, modified from Saria *et al.*, 2013 and Stamps *et al.*, 2018]. Green circles represent seismicity of the 1900–2020 catalogue (this study), open circles events with no magnitude. Focal mechanisms are from GCMT [Ekström *et al.*, 2012, Grimson and Chen, 1988, Foster and Jackson, 1998, Barth *et al.*, 2007, Craig *et al.*, 2011, Rakotondraibe *et al.*, 2020]. Black rectangle indicates limits of Figure 2. K, M and L are for Kerimbas and Majunga basins and Saint Lazare Seamounts, respectively. Years of occurrence are indicated for Mw 5.5+ events.

Although the origin of the volcanism is debated, the alignment of the islands of the Comoros archipelago, concentrating a significant part of the regional seismic activity, may correspond to localized strain at the scale of the width of the Mozambique Channel, linking the southern part of the EARS to extension in Madagascar [for instance Anokay–Alaotra basin and central and northern Madagascar volcanic fields; e.g., Laville *et al.*, 1998, Rufer *et al.*, 2014, Supplementary Figure S1]. The distribution and focal mechanisms of earthquakes are therefore crucial to better understand the transfer of deformation from the continental rifting occurring in southeastern Africa, and especially at the southern end of the EARS where the extensional rift structures are less clear and the seismicity more diffuse, to the volcanic and extensional region of Madagascar island characterized by moderate and regular seismicity [Bertil and Regnault, 1998]. Despite the sparseness of geologic and geodetic data in the region, it has been proposed that the archipelago outlines a boundary in the northern Mozambique Channel between the Lwandle and Somalia plates [Hartnady, 2002, Kusky *et al.*, 2007]. Kinematic markers of deformation, whether from geology or seismology (E–W dextral focal mechanisms) are compatible with such an interpretation [Famin *et al.*, 2020, Lemoine *et al.*, 2020a, Feuillet *et al.*, 2021]. The few geodetic data across the region have constrained various kinematic models. Some of them proposed that the region encompasses wide zones of diffuse deformation [Stamps *et al.*, 2018, 2020, Kusky *et al.*, 2010] or that the Lwandle/Somalia plate boundary is located either across the Mozambique Channel and Madagascar [Saria *et al.*, 2013] or further north along the Comoros archipelago [Stamps *et al.*, 2018]. In this latter model, the relative velocity of the plates along the ~E–W-trending axis of the archipelago is low, less than 1 mm/yr, and would correspond to right-lateral strike-slip transform faulting.

3. Historical seismicity

We have a very incomplete view of the historical seismicity of Mayotte and the Comoros. The most ancient information, gathered in Hachim [2004], is a set of testimonies collected from the population and based on oral memories transmitted over several generations. We thus go back as far as the 17th

century with four earthquakes that caused damage to the mosques of Mtsamboro (1606), Tsingoni (1679), Sada (1788) and Tsingono (1791). The location and magnitude of these earthquakes remain unverifiable. In 1829, Gevrey [1870] and Vienne [1900] mentioned damages due to telluric hazard, whereas Lambert [1997] attributed them to a cyclone. Earthquakes felt in Grande Comore were related to the volcanic activity of the Karthala volcano in 1808, 1858, 1865, 1880, 1904 and 1918 [Bachèlery *et al.*, 2016]. The magnitude 6 event of 23 August 1918 seems to have been the most violent earthquake felt by the population, since it was mentioned by the International Seismological Summary (ISS) and felt as far as Moheli [Lacroix, 1920] but without indications of damage or human casualties.

From the 1920s until 1960, the earthquakes felt in the Comoros and Mayotte were systematically reported by the Observatory of Tananarive and transcribed in the Bulletins of the Malagasy Academy and the *Annales de Physique du Globe de Strasbourg*. Earthquakes have regularly been felt in each of the islands. An earthquake was reported with moderate damage in Mayotte on 16 January 1936. The SISFRANCE-Océan Indien [2010] database locates the epicentre west of Mayotte. On 20 January 1953, another event was strongly felt in Moroni and observations of cracks on walls were reported [Boulanger, 1953].

Historical seismicity, although limited to a short period of time (less than 200 years for written records), shows that seismic events are a regular phenomenon in the Comoros islands. The existing reports testify to rare moderate damages on built structures without any mention of injured inhabitants. It is important to note that the analysis of the historical archive shows that no seismic sequence equivalent to that of 2018–2020 still going on in Mayotte occurred, although some seismic swarms of short duration (tens of days) have been observed on the flanks of Karthala in 1918 and 1953 [Lacroix, 1920, Boulanger, 1953].

4. Instrumental seismicity

4.1. Instrumental seismic networks

We have built a catalogue of the regional instrumental seismicity over the period 1900–2020 (Supplementary Table S1) for the region under study

(longitude 35° E–52° E, latitude 26° S–6° S; Figure 1), including Madagascar, Comoros, the Mozambique Channel and the East African coasts between Mozambique and Kenya. Working on such a large time period of observation implies that the evolution of the instrumental seismic monitoring is taken into account, in order to understand the evolution of the completeness of the datasets over time. We use two kinds of datasets to build this catalogue of the instrumental seismicity: a combination of existing catalogues established at regional or local scales over the last century, and the catalogue of BRGM for the recent 2016–2020 period.

4.1.1. *Evolution of seismic networks and bulletins*

For the first half of the 20th century, pioneering instrumentation was mostly installed in Europe and North America. The development of International Seismological Summary (ISS) since 1918 makes both the detection and the location of $M > 6$ possible over a large area of the world. However, detection of African earthquakes using European stations remains inhomogeneous over time with an inaccurate epicentral location.

The first worldwide seismograph array was installed in 1950. In 1964, the American World-Wide Standardized Seismograph Network (WWSSN) was fully operational and inspired the creation of many other national seismograph networks, improving the completeness of catalogues and the detection of moderate seismicity around the world. After 1985, simultaneous digital instrumentation development and associated time clocks led also to a considerable improvement in the accuracy of assessment of earthquakes locations. Those advances pushed forward the development of seismic arrays in Africa, with broadband stations belonging to worldwide networks and local short-period stations.

The large amount of seismological data is gathered in specialized consortiums, like the International Seismic Centre [ISC, Adams *et al.*, 1982, Bondár and Storchak, 2011], which archives, processes and distributes catalogues coming from international and regional arrays. ISC also leads research programmes [e.g., the Global Instrumental Earthquake Catalogue ISC-GEM, Storchak *et al.*, 2013] to digitize past paper seismographs, in order to re-build, gather and complete catalogues of the recorded seismicity before 1950, including in Africa.

4.1.2. *Evolution of regional seismic networks*

The whole region of the Mozambique Channel and Madagascar suffers from an insufficiently developed seismic network preventing a homogeneous detection of the regional seismicity. Not known as a strong seismicity-prone zone, the region has not been targeted for precursory seismic instrumentation. Furthermore, permanent instrumentation is difficult to maintain in those areas and homogeneous coverage of moderate seismicity in oceanic domains is challenging. Seismic activity in the Mozambique Channel is recorded by seismic networks in East Africa, in the Comoros archipelago and in Madagascar (Table 1).

Jesuits Company installed the first seismograph in Madagascar, near Antananarivo, in 1898. A local network of four stations equipped with short-period sensors was deployed in 1973 in the central part of Madagascar. Between 2007 and 2009, four additional broadband stations have been installed on the island: G.FOMA (Geoscope; Institut de Physique du Globe de Paris, IGP, and Ecole et Observatoire des Sciences de la Terre, EOST, 1982; DOI: 10.18715/GEOSCOPE.G), ILABPO (IRIS/IDA; Scripps Institution Of Oceanography, 1986, <https://doi.org/10.7914/SN/II>), GE.SBV and GE.VOI (GEOFON seismic network, GEOFON Data Centre, 1993, <https://doi.org/10.14470/TR560404>). Today, the permanent Malagasy seismic network counts seven short-period and four broadband stations.

Creation of the WWSSN drove the installation of a long and short-period seismic station in Kenya in 1963. A collaboration with GFZ (GeoForschungsZentrum in Potsdam, German Research Centre for Geosciences) allowed the installation of a local seismic network in 1990. Nowadays, one short-period and four broadband stations are operational in Kenya, including the GE.KIBK station which is the closest one to the Comoros archipelago.

The creation of the Observatoire Volcanique du Karthala (OVK) in 1986 motivated the installation of seismic stations around the Karthala volcano on the island of Grande Comore. Since 1988, four to eight short-period stations form the OVK seismic monitoring network, which has been complemented by four broadband seismic stations from 2017.

Despite recent developments, regional networks remain inhomogeneous in space and time to

Table 1. Seismic stations at regional distances (<1500 km) classified by increasing epicentral distance with respect to main earthquake of May 15, 2018; stations added after beginning of crisis between 2018 and 2019 are shaded

Network	Code	Start	End	Latitude	Longitude	Elevation	Place	Country	Type	Distance
AM	RCBF0	2018-06-25	05/07/2018	-12.7984	45.2748	11	Pamandzi	Mayotte-France	RaspB	31
1T	PMZI	2019-03-06		-12.7993	45.2743	10	Pamandzi	Mayotte-France	BB (HH)	31
RA	MDZA	2016-06-28	2019-02-28	-12.7825	45.2555	5	Dzaoudzi	Mayotte-France	Acc	33
RA	YTMZ	2016-06-28		-12.7557	45.2307	34	Mamoudzou	Mayotte-France	Acc	36
AM	ROCC5	2019-07-21		-12.7557	45.2307	34	Mamoudzou	Mayotte-France	RaspB	36
AM	RAE55	2018-06-27		-12.7335	45.2036	47	Koungou	Mayotte-France	RaspB	39
RA	MILA	2019-02-28		-12.8481	45.1928	30	Dembeni	Mayotte-France	Acc	41
AM	R1EE2	2019-07-17		-12.8354	45.1365	113	Coconi	Mayotte-France	RaspB	47
ED	MCHI	2018-06-23		-12.8329	45.1237	130	Chiconi	Mayotte-France	BB (BH)	48
1T	MTSB	2019-03-07		-12.6804	45.0847	50	Mtsamboro	Mayotte-France	BB (HH)	52
QM	KNKL	2019-03-04		-12.9571	45.1042	24	Kani-Keli	Mayotte-France	BB (HH)	54
KA	KANG	2020-07-24		-12.3046	44.4679	913	Kangani	Comores	BB (HH)	129
QM	GGLO	2019-03-13		-11.5830	47.2924	7	Grande Glorieuse	Glorieuses-France	BB (HH)	230
KA	DEMB	2017-05-04		-11.8774	43.4062	300	Dembeni	Comores	BB (HH)	254
KA	CAB	2017-12-02		-11.7486	43.3435	1984	Cabanes	Comores	BB (HH)	266
KA	MOIN	2017-05-04		-11.7660	43.2435	145	Moindzaza	Comores	BB (HH)	276
KA	SBC	2006-13-01		-11.6491	43.2969	640	Bahani	Comores	BB (HH)	276
GE	SBV	2009-11-19		-13.4584	49.9212	65	Sambava	Madagascar	BB (HH)	477
II	ABPO	2007-04-04		-19.0180	47.2290	1528	Ambohipanombo	Madagascar	BB (HH)	716
GE	VOI	2009-11-26		-21.9065	46.7933	1158	Vohitsoka	Madagascar	BB (HH)	1023
G	FOMA	2008-09-01		-24.9757	46.9789	28	Fort Dauphin	Madagascar	BB (HH)	1364
G	RER	1986-02-10		-21.1712	55.7399	834	Sainte-Rose	Réunion-France	BB (HH)	1409
II	MSEY	1995-05-15		-4.6737	55.4792	475	Mahe	Seychelles	BB (HH)	1420
GE	KIBK	2011-09-13		-2.3591	38.0433	790	Kibwezi	Kenya	BB (HH)	1426

Station types: Acc = accelerometer, BB (HH) broadband 0–100 Hz, BB (BH) broadband (0–50 Hz), RaspB: Raspberry Shakes. Networks: AM: Raspberry Shakes: <https://doi.org/10.7914/SN/AM>; ED: <http://www.edusismo.org/>; G: Geoscope: doi:10.18715/GEOSCOPE.G; GE: GEOFON: doi:10.14470/TR560404; II: GSN IRIS-IDA: <https://doi.org/10.7914/SN/II>; KA: OVK: <http://www.cndrs-comores.org/observatoires/ovk/>; RA: RESIF-RAP: doi:10.15778/RESIFRA, 1T, QM: CNRS-INSU Tellus SISMA YOTTE project.

continuously and consistently monitor the regional seismicity.

4.1.3. Mayotte network

In Mayotte, in the framework of the Résif-RAP [RESIF, 1995, <http://dx.doi.org/10.15778/RESIFRA>], BRGM operates three strong motion stations: two continuous stations, RA.YTMZ since June 2016 and RA.MILA since March 2019, one triggered station, RA.MDZA between 2016 and February 2019. Since June 2019, the monitoring of the seismo-volcanic activity in the Mayotte region has been entrusted to the “Mayotte Volcanic and Seismic Monitoring Network” (REVOSIMA, <https://www.ipgp.fr/fr/revosima/reseau-de-surveillance-volcanologique-sismologique-de-mayotte>). IGP operates this network through the “Observatoire volcanologique du Piton de la Fournaise” (OVPF-IPGP) in La Réunion, in co-responsibility with the BRGM (French Geological Survey) and its regional direction in Mayotte.

With the onset of the seismo-volcano-tectonic sequence near Mayotte in May 2018, and the need to record and localize the close moderate-to-strong and unusual seismic activity, the monitoring network grew significantly. Three new stations have been installed before the end of June 2018: AM.RAE55 and AM.RCBF0 (1D and 3D Raspberry Shake station, respectively, RCBF0 was operational only for two weeks) integrated to the Raspberry Shake network (Raspberry Shake Community, 2016, <https://doi.org/10.7914/SN/AM>), and the first broadband station on the island ED.MCHI belonging to the French educative network (www.sciencesalecole.org/plan-sismos-a-lecole-presentation). In March 2019 four new broadband seismic stations were installed: QM.KNKL, 1T.MTSB and 1T.PMZI in Mayotte, and QM.GGLO in Grande Glorieuse island (QM network code for Comoros Seismic Network; 1T for the temporary seismological network of Mayotte). Then the most recent improvement of the inland network was the addition of AM.R1EE2 and AM.ROCC5

(3D Raspberry Shake stations; AM.R0CC5 being at the same location than RA.YTMZ). Therefore, from August 2019, eight stations for a total of eleven sensors are operating in Mayotte: four broadband stations, among which two are equipped with a strong motion sensor as well, two accelerometers including one co-located with a Raspberry Shake, and two Raspberry Shakes. Despite the improvement of the monitoring network, the detection and the location of the seismic activity are highly constrained by the local environment inducing noisy seismic signals. Many of the stations are installed in small coastal urban areas, with a variable detection threshold between night and day in addition to the noise from the ocean.

4.2. Seismicity catalogue

Most of the data acquired by the regional networks are not distributed and the waveforms cannot be easily used to reprocess hypocentral locations. For this reason, most of the events of our regional catalogue (Supplementary Table S1) are gathered from existing catalogues.

4.2.1. Existing catalogues for the whole region

Since the regional seismic networks were developed only recently in the Comoros archipelago and its vicinity, local catalogues are primarily built using worldwide instrumentation. As a consequence, the number of events is highly dependent on the improvement of the worldwide instrumentation and the progressive installation of the regional networks, as described above.

Before 1950, the 13 seismic events of our catalogue came from the old seismological summaries [Gutenberg and Richter, 1954; bulletins from the International Seismological Summary, 1918–1963] and reviews of instrumental or macroseismic events [Bath, 1975, Ambraseys and Adams, 1991; ISC-GEM Di Giacomo *et al.*, 2015a,b, 2018, SISFRANCE-Océan Indien, 2010].

After 1950, our catalogue benefits from the International Seismological Centre archives [ISC, International Seismological Centre, 2021, Bondár and Storchak, 2011], incorporating data from multiple growing regional African arrays: NAI (Kenya), TANZ (Tanzania), LSZ (Zambia), BGSi (Botswana), BUL (Zimbabwe), CNG (Mozambique before 1968), JOH

and PRE (South Africa), EAF (East Africa network, comprising stations from Ethiopia, Kenya, Malawi, Uganda, Zambia and Zimbabwe). These data correspond mainly to the seismic activity occurring in the western part of the Mozambique Channel and form the basis of our catalogue from 1950 to 2020. We complete our dataset with regional events located in the framework of specific regional studies not included in ISC. Malagasy network provides information on the seismic activity affecting the eastern part of the Mozambique Channel. Data of the 1973–1976 period come from the first locations of the Malagasy network [Rakotondrainibe, 1977]. Then, a large part of our dataset in Madagascar and Mozambique Channel comes from the 1978–1995 catalogue compiled by Bertil and Regnoul [1998]. The hypocentral locations outside Madagascar Island are all at a fixed depth of 16 km. We also include the Rakotondraibe *et al.* [2020] Malagasy seismic catalogue (October 2011–August 2013) built from temporary networks in the island.

Regional reviews of seismicity complement the worldwide catalogue. For the beginning of the instrumental period, we note the catalogue compiled by Sykes and Landisman [1964]. This study combines arrival times from various catalogues of the Red Sea, East Africa, Oman and Arabian regions, and slightly increases the number of earthquakes detected in the Mozambique Channel and Tanzania between January 1955 and March 1964. The catalogue compiled by Bath [1975] on the instrumented seismicity of Tanzania complements the dataset from 1910 to 1974 in this area.

4.2.2. BRGM seismicity catalogue of Mayotte 2016–1/10/2020

From May 2018 to May 2019, the Mayotte seismic sequence was monitored by a small number of local and regional stations (see Section 4.1.2), and a progressively increasing number of new stations on the island installed between June 2018 and March 2019 (see Section 4.1.3). A seismicity catalogue of this sequence has been published by Lemoine *et al.* [2020a], based on the initial detections of Bertil *et al.* [2019], using a localization process with HYPO71 [Lee and Valdes, 1985] and a 1D regional velocity model (Table 3). The estimated magnitude is a local magnitude M_{lv} . In order to remain homogeneous over the

whole 2018–2020 period, we followed the same localization process to complement this catalogue from May 2019 to October 2020 with the events of magnitude above 3.5 (M_{lv}) in Mayotte. In addition, the locations from May to August 2018 have been updated using additional phase arrival times [Mercury *et al.*, 2020]. This results in 1938 located hypocentres whose 3D spatial distribution (Supplementary Table S1) is consistent with the locations calculated after February 2019 by MAYOBS-REVOSIMA using new Mayotte stations and offshore OBS [Lemoine *et al.*, 2019, Saurel *et al.*, 2019, 2021].

This catalogue is extended to the earthquakes between the coasts of Mozambique and northwest Madagascar located between 2016 and 2020, using HYPO71 and the same velocity model. This allows the addition of 92 regional events not reported by ISC.

4.2.3. Magnitude homogenization of the catalogue

Because our dataset comes from various distinct catalogues, several criteria have been applied to homogenize our final catalogue (Supplementary Table S1). By default, the locations are those given by the ISC catalogue.

- Before 1964, in case of duplicates, the most recent location is kept [ISC-GEM; Sykes and Landisman, 1964, Bath, 1975; articles].
- Between 1964 and 2016, duplicates only concern the catalogues of Madagascar [Rakotondrainibe, 1977, Bertil and Regnault, 1998, Rakotondraibe *et al.*, 2020] and correspond to events with magnitude higher than 5 before 2010, and higher than 4.5 between 2010 and 2016. We choose to keep the ISC-GEM or ISC location.
- For the 2016–2020 period, duplicates concern mainly events located between the Davie Ridge and northwestern Madagascar. We choose to keep the locations determined from regional networks (see Section 4.2.2).

Also, because the catalogues include various types of magnitudes M_w , m_b , M_s , M_l , M_d , we use the magnitude M_w for all the events, following the priority order below:

- When available, we attribute M_w from ISC-GEM or by Global Centroid-Moment Tensors [GCMT, Dziewonski *et al.*, 1981, Ekström *et al.*, 2012].

- When available, we use M_w from regional studies [Grimison and Chen, 1988, Barth *et al.*, 2007].
- If magnitude is expressed by m_b , we convert m_b to M_w following the relation established by Scordilis [2006]: $M_w = 0.85 * m_b + 1.03$.
- If magnitude is expressed by M_{lvBRGM} , M_{lvBRGM} is converted to M_w using $M_w = M_{lvBRGM} - 0.4$. This conversion is based on an empirical relation between M_{lvBRGM} and M_{wGCMT} for 29 available events with $M_w \geq 5.0$.

For all the other datasets, because of lack of pre-established or easily estimated relation, we consider that M_l or M_d magnitude equals M_w . This corresponds to 1324 events of our dataset. The resulting catalogue contains 5393 events of which 5359 have an estimated magnitude (Supplementary Table S1).

4.3. Focal mechanisms

A few focal mechanisms are available for the study area (Supplementary Table S2). We compile the focal mechanisms from the GCMT catalogue for the period 1976–2020 [Dziewonski *et al.*, 1981, Ekström *et al.*, 2012] and from seismotectonic studies pursued in the region [Grimison and Chen, 1988, Foster and Jackson, 1998, Barth *et al.*, 2007, Craig *et al.*, 2011, Rakotondraibe *et al.*, 2020]. This accounts for 107 events for the region including Madagascar, Comoros archipelago, Mozambique Channel up to the east coast of Africa, with 28 of them belonging to the Mayotte sequence from 14/05/2018 to 02/01/2020 (Figures 1–3).

Most of the focal mechanisms are consistent with normal faulting, striking N–S along the Davie Ridge, along the coast of Tanzania or across Madagascar. Normal faulting along WNW–ESE to NW–SE-trending planes are observed around the Comoros archipelago. Pure strike-slip events or normal faulting events with a strike-slip component are also observed, particularly during the Mayotte seismic sequence [with tensional axis oriented NE–SW, Lemoine *et al.*, 2020a], along the Comoros archipelago or within the Mozambique Channel. Only a few thrust faulting mechanisms are reported. We note the event of 14/05/2019 (M_w 4.9, Figure 3) belonging to the Mayotte seismic sequence.

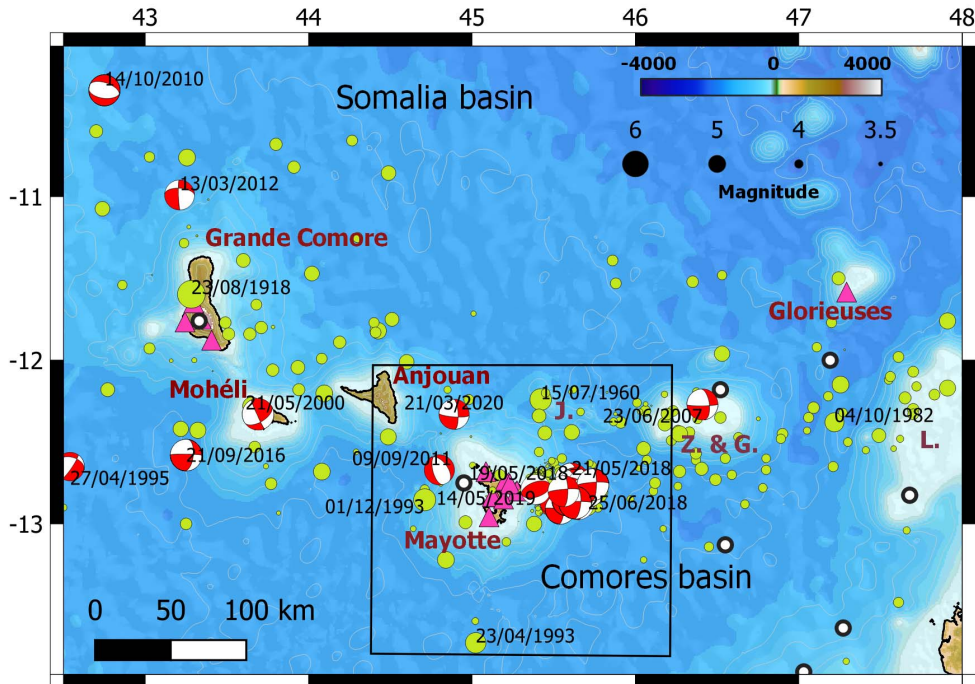


Figure 2. Seismicity in the Comoros archipelago (legend same as in Figure 1). Pink triangles are seismic stations. Years of occurrence are indicated for Mw 5+ earthquakes. Z. & G.: Zélée and Geyser bank; L: Leven bank; J: the Jumelles volcanic ridges. Black rectangle is Figure 3.

5. Results: regional seismicity

5.1. Evolution of detection threshold for the Comoros

The instrumental detection threshold for earthquakes in the Comoros area (within the limits defined in Figure 2) remained high, 5.5 to 6.0, up to late 1970s (Figure 5). Whereas the strongly felt and with reported damages earthquakes of 1936 (Mayotte) and 1953 (Grande Comore) have not been detected by the existing instruments, those of 23 August 1918 (Grande Comore) and July 1960 (northeast Mayotte) have been detected but without reliable assessment of their magnitude (Figure 3).

In our homogenized catalogue, nine earthquakes have Mw \geq 5.0 between 1982 and the beginning of the seismic sequence in 2018. The strongest one (Mw = 5.5) took place offshore, west of the coasts of Mayotte on 1 December 1993.

Using the catalogue compiled by Bertil and Regnault [1998], the detection threshold decreases to 4.0 for the period 1978–1995. Even if there is an

improvement in the detection by international networks, without the Malagasy network, the detection threshold remains beyond Mw 4.5 until 2016 (Figure 5, Table 2). Because of the strong motion stations installed in Mayotte, the OVK stations, and eventually the monitoring network dedicated to the sequence in Mayotte from 2018, detection threshold drops to Mw 3.5 for the whole region and below 3.0 around Mayotte from 2016.

5.2. Spatial and temporal distribution of seismicity

Despite its limitations, our new regional seismicity catalogue brings crucial constraints to characterize the seismicity and its evolution at regional scale (Figure 1; Supplementary Table S1).

Overall, seismicity along the southeast margin of Africa, along the Davie Ridge and across the Mozambique Channel towards the Mozambique Ridge is associated with rifting, N–S normal faulting along the Davie Ridge and conjugate normal faults in the rift of the Mozambique Basin. Seismicity in the Comoros

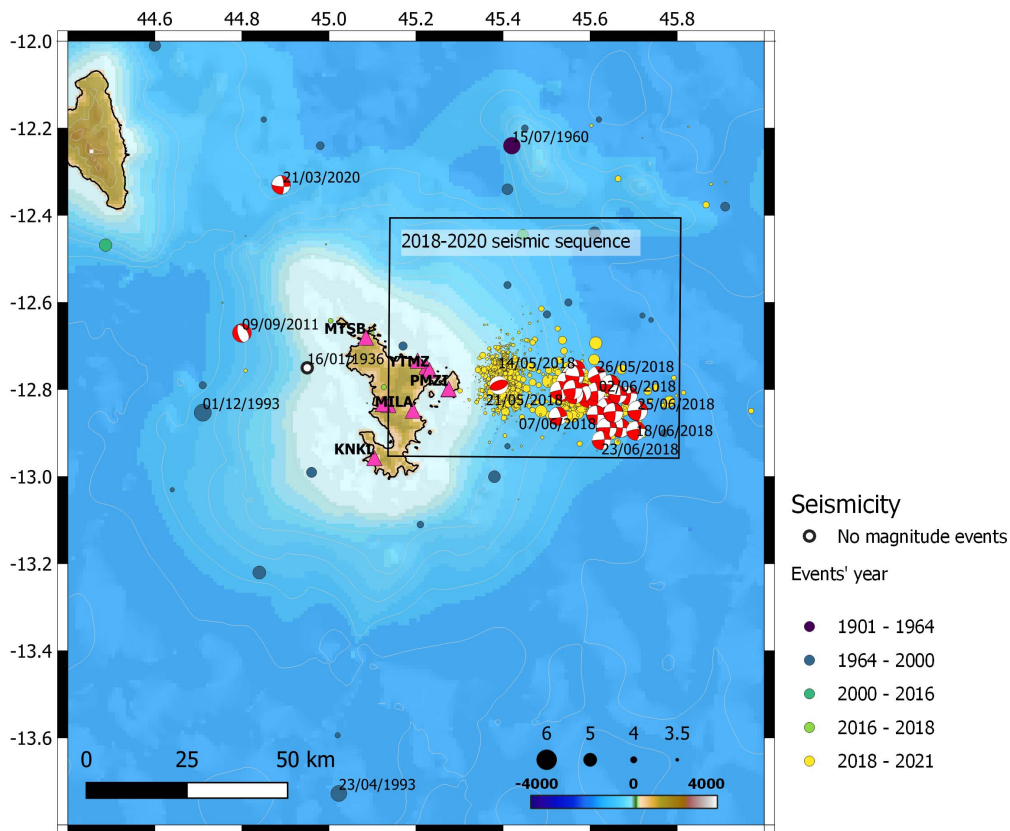


Figure 3. Seismicity around Mayotte. Dates for events with Mw 5+, excluding events of 2018–2020 Mayotte seismo-volcanic sequence. Focal mechanisms are from GCMT. Black rectangle is Figure 4.

Table 2. Periods of completeness for Comoros area (42.5° E–48.0° E, 14.0° S–10° S)

Years	Mc
1910–1979	6.0
1980–1995	4.0
1996–2009	4.7
2010–2016	4.5
2016–2020	3.5

Table 3. Velocity model used for 2018–2020 Mayotte sequence and for 2016–2020 regional seismicity

Layer top (km)	V (km/s)
3	3.5
8	5.1
15	6.7
	8.1
VP/VS	1.74

remains diffuse but underlines the broad trend of the archipelago. In the next sections, we describe the seismic activity taking into account the volcanic and tectonic knowledge in each seismic area.

5.2.1. Southeastern Tanzania

The East African Rift System (EARS) corresponds to the major extensional system crossing the African continent from the Horn of Africa to the south over more than 3000 km. The extensional deformation and the volcanism are concentrated along two main branches, the western branch and the eastern branch [Chorowicz, 2005], which are well developed on both sides of the Victoria microplate. South of this microplate, whereas the western branch of the EARS continues onshore and southward to western Mozambique and Okavango (Botswana), the eastern branch can be prolonged to the south towards the Tanzanian divergence [Tiberi *et al.*, 2019]. The

tectonic extensional structures and volcanism border the eastern edge of the Tanzanian craton forming the south of the Victoria plate, when another axis of tectonic deformation, sometimes called the “third branch” of the EARS, corresponds to the onshore Pangani rift in addition to a region in Southeastern Tanzania affected by an early stage of extension [Noble *et al.*, 1997, Le Gall *et al.*, 2004]. At present, the deformation of this region is slow, even though it is affected by a diffuse seismicity. Along the Northern Tanzanian rift, at the southern end of the eastern branch of the East African Rift System, the seismicity is characterized by sequences of seismicity including deep and shallow hypocentres [Albaric *et al.*, 2010]. Even though the event of 2007, with a magnitude Mw of 5.6 and whose focal mechanism shows normal faulting along NE–SW-trending planes, is the main event of the seismo-volcanic sequence [Calais *et al.*, 2008] affecting the upper crustal layer in the vicinity of the Oldoinyo Lengai and Gelai volcanic edifices, deep lithospheric structures involved in the continental rifting can also be activated [Albaric *et al.*, 2010]. Further east, the “third branch” continues offshore along the coasts of Tanzania and Mozambique, where the seismicity is less diffuse and forms a belt. The focal mechanisms are consistent with an ~EW-trending extension.

5.2.2. *Kerimbas basin*

The Kerimbas basin is a NS-elongated 30–40-km-wide active graben located 100 km off the coasts of Tanzania and Mozambique between 8° S in the north and 13° S near the St Lazare volcanic seamount [e.g., Mougénot *et al.*, 1986, Franke *et al.*, 2015]. Seismicity in and around the graben is mostly concentrated at the location of the 1985 seismic sequence, i.e. westward from the axis formed by the Comoros archipelago [Grimison and Chen, 1988], and south of the St Lazare seamount. Some diffuse seismicity occurs between the coast and the western shoulder of the basin (Figure 1). The 1985 Kerimbas seismic sequence encompasses some of the largest events of the region after the 1901 Mw 7 onshore Tanzania event [Ambraseys and Adams, 1991]. On 14 May 1985, two events of magnitude Mw 6.0 and Mw 6.4 occurred in a time window of 5 h at the same location [–10.59° S, 41.37° E and –10.49° S, 41.43° E; Grimison and Chen, 1988]. Despite the uncertainties of their absolute locations, they occurred along the

northern half of the eastern border faults of the Kerimbas graben [Franke *et al.*, 2015; Figure 1]. The focal mechanisms confirm this observation, since they indicate dip-slip normal faulting on N350 strike and 45° dip plane, subparallel to the well-expressed morphology of the bathymetric scarps [Franke *et al.*, 2015]. These events were followed by numerous aftershocks of magnitude 5–5.5 with similar mechanisms, and a specific seismic activity is regularly observed since then in this area, with three large events in 2005 (Mw 5.2), 2008 (Mw 5.7) and 2016 (Mw 5.1).

Before the 1985 sequence, magnitude 5 events occurred in 1976 and 1982, while seismicity below magnitude 5 was spread between the graben and the coast. Some seismicity is observed south of the St Lazare seamount (events of 1979, Mw 5.2 and 1995, Mw 5.3) with mostly north–south normal fault mechanisms. Diffuse seismicity is distributed between the Kerimbas graben and Grande Comore island (Figure 1). Three events of magnitude 5 occurred in 18/06/2007, 16/09/2007 and 14/10/2010. Their focal mechanisms are consistent with normal faulting along E–W to NW–SE striking planes.

5.2.3. *Mozambique Channel and Mozambique Basin*

To the south of the Kerimbas graben, the seismicity is broadly aligned along the ~NS-trending Davie Ridge between 13° S to 19° S and follows a NE–SW direction in the middle of the Mozambique Basin towards the Mozambique Ridge from 19° S to the south (Figure 1). Before 1960, the ISC catalogue encompasses about seven events of magnitude above 6.0, four of them located within this seismicity belt (1915, M6.4; 1938, M6.1; 1950 M6.2; 1951, M6.1), one of them in the middle of the eastern Mozambique Basin (1919, M6.1) and two of them along the coasts of Madagascar (1943 M6.1; 1952, M6). We note that the epicentres of the 1938 and 1951 earthquakes have been located in the same area where the Mw 5.6–5.7 main event of 24/09/2006 occurred. The latter was followed by many aftershocks and with focal mechanisms consistent with normal faulting along N175° E striking plane, i.e. subparallel to the overall strike of the Davie Ridge and the fault scarps outlined in the bathymetry [Courgeon *et al.*, 2018, Deville *et al.*, 2018].

Near the latitude 15–16° S, three events of magnitude 4.8–5.1 are located along and east of the Davie Ridge, in the vicinity of the 1950 Mw = 6.1 event,

whose focal mechanism shows strike slip faulting along NNE–SSW/WNW–ESE-trending planes, with a corresponding tensional axis compatible with the surrounding normal faulting events.

5.2.4. *Karthala volcano in Grande Comore*

Most of the seismicity located in Grande Comore is associated with the eruptions of the Karthala volcano (Figure 2). The Karthala volcano has erupted every 8–12 years on average since the middle of the 19th century and the last eruption dates back to January 2007 [Bachèlery *et al.*, 2016]. In the recent period, the eruptions of 1977, 1991, and 2005 to 2007 were accompanied by earthquakes felt by the population but not detected by the international networks because the magnitudes remain smaller than 4.5–5.0. For the 1991 eruption, the OVK observed earthquakes with a magnitude up to $M_l = 4.3$ [Savin *et al.*, 2005], and the seismic network of Madagascar detected only the strong events, with magnitudes M_l ranging from 3.8 to 4.3 (converted to M_w 4.3–4.6 in our catalogue).

Two seismo-volcanic sequences are remarkable. The first one occurred in August 1918, with a strong earthquake felt up to Moheli on 23 August 1918 and other strong shocks felt two days later. This sequence was associated with a phreatic eruption and a summit collapse [Lacroix, 1920, Bachèlery *et al.*, 2016]. Worldwide seismographs captured the tremor of the former, suggesting a magnitude above 6.0. The newspapers of the colony of Madagascar mentioned with fright these tremors as strongly felt, but neither indicate victims nor describe consequent damages. The second seismo-volcanic sequence occurred in January–February 1953, and the strong seismic activity worried the population and caused moderate damage to buildings. A comprehensive macroseismic report was made at the time [Boulanger, 1953]. The main earthquake of 20 January 1953 would have produced intensity VII in Moroni (rather VI on an EMS98 scale). It was preceded the same day by 28 felt tremors [Boulanger, 1953]. The epicentre is located on the western flank of Karthala (towards the city of Boboni) and the main shock is shallow (depth of ~2–3 km). Worldwide networks did not detect the main shock and its magnitude remains unknown. Events are reported until 3 February 1953. No aerial volcanic eruption has been observed and the sequence is likely a crustal magmatic intrusion that did not reach the surface.

Despite the occurrence of significant earthquakes at Karthala, no seismic swarms comparable in duration and number of large shocks as during the current Mayotte sequence were observed since at least the 19th century.

5.2.5. *Mayotte and western Comoros archipelago*

Across the Comoros (Figure 2), the seismicity is spread over a vast 500-km-long and 200-km-wide zone, from Grande Comore at 43° E to the Leven bank at 48° E. From West Mayotte (44.5° E) to the Leven Bank, the seismicity forms a narrower 350-km-long and 70-km-wide band. West of Mayotte (between 43° E and 44.5° E) and in the vicinity of the islands of Anjouan, Moheli and Grande Comore, the seismicity appears to be more diffuse. While most of the earthquakes remain fairly close to the islands, a few of them are localized both in the Somalia Basin (such as the 14/10/2010 M_w 5.2 normal faulting event more than 120 km north of Grande Comore, Figure 2) and in the Comoros Basin (such as the 23/04/1993 M_w 5.4 event located 80 km south of Mayotte, Figure 2; and the 29/04/1952 M_w 6.0 event located more than 250 km south of the archipelago, Figure 1).

The strongest earthquakes observed have a magnitude above 5.0. Nine of them occurred between 1982 and 2020. In comparison, up to 30 events with $M \geq 5.0$ occurred during the 2018–2020 Mayotte sequence. The earthquake of 15 July 1960 is located 70 km northeast of Mayotte, close to the two sub-parallel Jumelles volcanic ridges [Tzevahirtzian *et al.*, 2021 and Figure 2]. This event has been detected by 140 stations of the worldwide network but its magnitude has not been clearly estimated. However, both the number of records and the fact that it was widely felt in Mayotte, *i.e.* more than 70 km away, suggest a magnitude greater than 5.0. We note that some of these magnitude ≥ 5 earthquakes are accompanied by aftershock sequences such as the 2016 event in Moheli. No clear seismo-volcanic swarm behaviour is observed.

Mayotte is at the centre of this zone of diffuse seismicity, since strong felt tremors are located in the west (earthquakes of 1936, 1993, 2011), the northwest (2020), the northeast (1960), the east (2018–2021 sequence), and even the south (1993) (Figure 3). Tectonic structures related to these earthquakes remain unknown up to now [Thinon *et al.*, 2020].

Five events have strike-slip focal mechanisms with N80°–100° E and NS-trending nodal planes, which is very similar to most of the mechanisms determined for the magnitude 5 events of the 2018–2021 Mayotte sequence, and particularly its main Mw 5.9 shock (Figure 4; see Section 5.3 below). Two events have normal fault focal mechanisms with NNW-SSE-trending or E–W-trending nodal planes.

5.2.6. Madagascar

The located seismicity in Madagascar is spread all over the island (Figures 1 and S1). The seismicity in its central part is well detected and located because the short-period network of the Observatory of Tananarive is installed in this area. In the northern and the southern parts of the island, the detection threshold remains higher than 4.4, even after the installation of the broadband stations SBV, ABPO, VOI and FOMA (Table 1, see Section 4.1.2).

The strongest known earthquake occurred on 29/03/1943 (Mw = 6) on the west coast of the island (Figure 1). This earthquake seems to be isolated, outside the active seismic zones detected so far. Over the 1980–2020 period, ten earthquakes of Mw ≥ 5.0 occurred in Madagascar and its surrounding areas, while eight Mw ≥ 5.0 events occurred along the Comoros–Geyser–Leven banks zone over the same period, excluding the specific seismo-volcanic swarm near Mayotte.

In the north of Madagascar, the seismicity is broadly distributed in the Baie d'Antongil-Nosy-Be ~N140–160-trending axis, where Neogene and Quaternary volcanics outcrop [Bertil and Regnault, 1998, Rufer *et al.*, 2014; Figure S1]. Together with the large Miocene stratovolcano of Massif d'Ambre that forms the northern Madagascar peninsula [Cucciniello *et al.*, 2011], this seismo-volcanic zone represents the easternmost expression of seismicity and volcanism at the eastern end of the Comoros archipelago. Overall, even in the absence of a continuous structure across Madagascar, it is tempting to delineate an active, segmented, mostly extensional zone from the province in the north to the Bekily region in the south, through the Anokay–Alaotra graben and the Ankaratra volcanic field and associated seismicity [e.g., Kusky *et al.*, 2007, Rakotondraibe *et al.*, 2020]. Although the kinematics of such a discontinuous structure remains to be determined, it may act as a boundary between the Lwandle microplate to the

west and the Somalia plate to the east, and as such, as the easternmost expression of the EARS.

5.3. The 2018–2020 Mayotte seismo-volcanic sequence

After the Mw 4 event that occurred on 10 May 2018 40 km east of Mayotte at the onset of the unexpected long seismo-volcanic sequence [Figures 3 and 4; Bertil *et al.*, 2019, Lemoine *et al.*, 2020a], the following earthquakes were distributed into two clusters, cluster A and cluster B (Figures 5 and 6).

Cluster A is located 40 km east of Mayotte, and encompasses all the earthquakes of the first two months of the sequence (mid-May to mid-July 2018). By including all the strongest events (32 events with a magnitude above 5.0), more than 80% of the total cumulative seismic moment of the whole sequence was released within the cluster A (Figure 6a). During the first four months, our catalogue contains 365 earthquakes and three main temporal phases can be identified corresponding to the onset of the Mayotte sequence.

First, from 10 May to the end of May 2018, a total of 40 events have been felt with 11 $M > 5$ events. The strongest event (Mw 5.9) of the whole sequence occurred on 15 May 2018 after five earthquakes of Mw > 4 of the first Mw > 5 event on 14 May 2018.

Second, during the first half of June 2018, the seismicity was the most intense, in terms of frequency and magnitude, with more than 60 felt earthquakes including 12 Mw 5+ events in less than two weeks.

Third, from mid-June to end of September 2018, strong activity resumed with an average of one felt (M4+) earthquake per day, including four M5+, over 20 days. The 27 June 2018 earthquake is the last M5+ until January 2020, and subsequent seismic activity remained low with only one M4+ event recorded until mid-August. The last burst of cluster A occurred over the whole month of September 2018, with ~120 events, including 30 events above M3.5 and two M4+ events.

Finally, from October 2018 to October 2020, cluster A is regularly active, with a slow decrease in its seismic activity from April 2019 (Figure 6b, 148 earthquakes from October 2018 to October 2019, and only 35 earthquakes from October 2019 to October 2020). From June 2020, the Mw > 3 earthquakes of the whole area belong to cluster A.

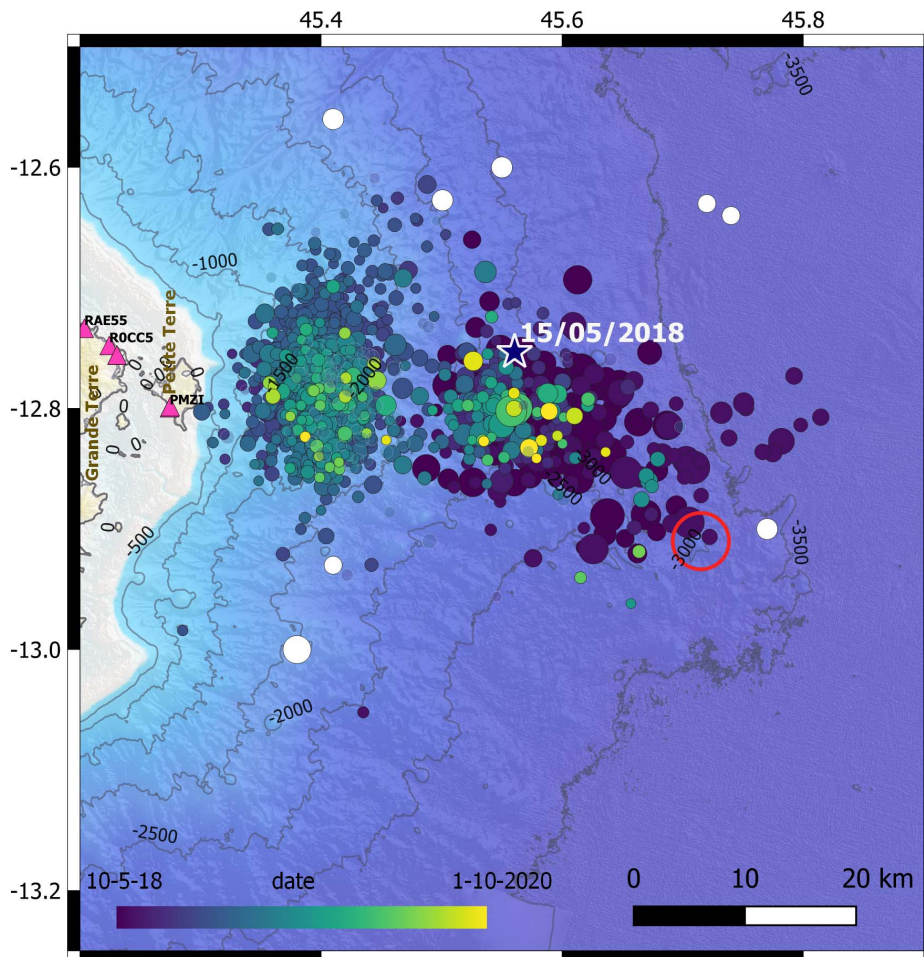


Figure 4. Mw 3.1+ (Mlv 3.5+) events of 2018–2020 Mayotte seismic sequence. Star is Mw 5.9 largest event of the sequence (15/05/2018). Red circle is new submarine volcanic edifice [Feuillet *et al.*, 2021]. White circles represent earthquakes preceding the 2018–2020 Mayotte seismic sequence. Bathymetry compiled in Lemoine *et al.* [2020b] from data in SHOM HOMONIM, Audru *et al.* [2006] and Feuillet *et al.* [2021].

The hypocentres belonging to cluster A are located at a depth ranging from 20 to 45 km, northwest of the new volcanic edifice (Figure 4) discovered in 2019, 50 km east of Mayotte [Feuillet *et al.*, 2019a, 2021, Deplus *et al.*, 2019].

Cluster B became active in August 2018, with the occurrence of low magnitude events (3 to 3.7; Figures 5 and 6b). While the activity slightly decreased in September when the last burst of the cluster A occurred, it became dominant from October 2018 to September 2019, with many earthquakes felt but with magnitude below 5.0. The largest earthquake (Mw = 4.9) oc-

curred on 14 May 2019, rather at the end of the most active period. For the cluster B, the catalogue encompasses a total of 1330 earthquakes from August 2018 to September 2019, and 54 events from October 2019 to October 2020.

A remarkable characteristic of the Mayotte seismic sequence is that the recorded seismicity is deep, distributed from 20 to 50 km [Jacques *et al.*, 2019, Feuillet *et al.*, 2021, Saurel *et al.*, 2021], i.e. below the estimated Moho depth around 20 km [Barruol *et al.*, 2018]. For the May–June 2018 period, Cesca *et al.* [2020] interpret the seismicity migration as the propagation of a magmatic dyke through

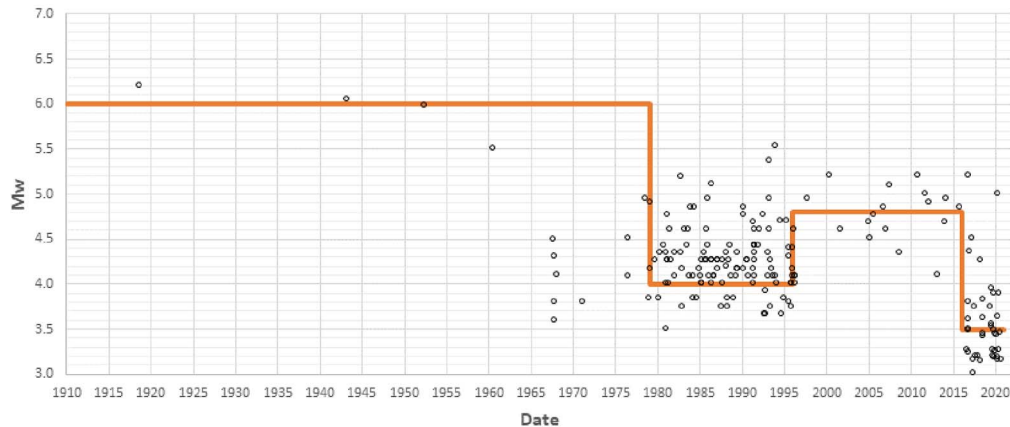


Figure 5. Magnitude distribution for Mw 3.0+ events for 1900–2020 regional catalogue (this study), excluding the events of Mayotte 2018–2020 sequence. Red dots are earthquakes of 1936, 1953, 1960 without estimation of magnitude but assumed to be above ≥ 5.0 . Orange line is detection threshold in magnitude.

the whole crust followed by the draining of a large, sub-Moho magma reservoir. Combining seismic and GNSS data, Lemoine *et al.* [2020a] proposed that the evolution of the seismic activity corresponds first to the fracturing of the crust, followed by the ascent of magma from a deep magma reservoir leading to the eruptive period. The significant subsidence in Mayotte is consistent with the deflation of a large and deep magma reservoir since the beginning of the eruption [Briole, 2018], possibly involving a small secondary source [Lemoine *et al.*, 2020a].

Since the discovery of the new volcanic edifice on the seafloor eastward offshore of Mayotte [Feuillet *et al.*, 2019b, 2021], several marine surveys have been conducted in order to deploy and retrieve ocean bottom seismometers (OBS) from late February 2019 and monitor the volcanic activity, and particularly that of the eruption which was still active in October 2020 (Revosima bulletin n° 27 and MAYOBS 15 doi:10.18142/291). The use of the data acquired by such networks are crucial for accurate hypocentral locations from the end of February 2019 [Saurel *et al.*, 2021, Lavayssière *et al.*, 2020, Hoste-Colomer *et al.*, 2020]. However, we did not include the locations from OBS data in this present study. Nevertheless, we present an homogeneous M3.5+ catalogue built from available data acquired by onshore regional and local stations. Mercury *et al.* [2020] initiated a more exhaustive analysis of the first weeks of the sequence that will help conduct a much finer

analysis of the distinct phases of the onset of the eruption.

Unusual Very Long Period (VLP) signals have also been observed throughout the sequence. An exceptional event occurred on 11 November 2018: a long-lasting monochromatic VLP, recorded worldwide, showing a decaying oscillation associated with a period of oscillations of ~ 16 s [Poli *et al.*, 2019, Satriano *et al.*, 2019, Cesca *et al.*, 2020, Laurent *et al.*, 2020, Lemoine *et al.*, 2020a]. Cesca *et al.* [2020] reported more than 400 of such VLP events during the first year of the Mayotte seismo-volcanic sequence. Some small events can be embedded within such signals. VLP events may attest to magmatic processes, however, their interpretation is outside the ambit of the present paper and their locations are not included in this catalogue. According to Laurent *et al.* [2020] epicentral locations of VLP events are 20 km east of Petite Terre, i.e. in the vicinity of seismic cluster B.

6. Discussion

6.1. Network evolution and catalogue

The catalogue presented in this study covers 120 years of seismicity within the Mozambique Channel and the Comoros archipelago, while the very recent evolution of the regional network offer the opportunity to get a refined image of the space–time distribution of the seismicity in this region. With the

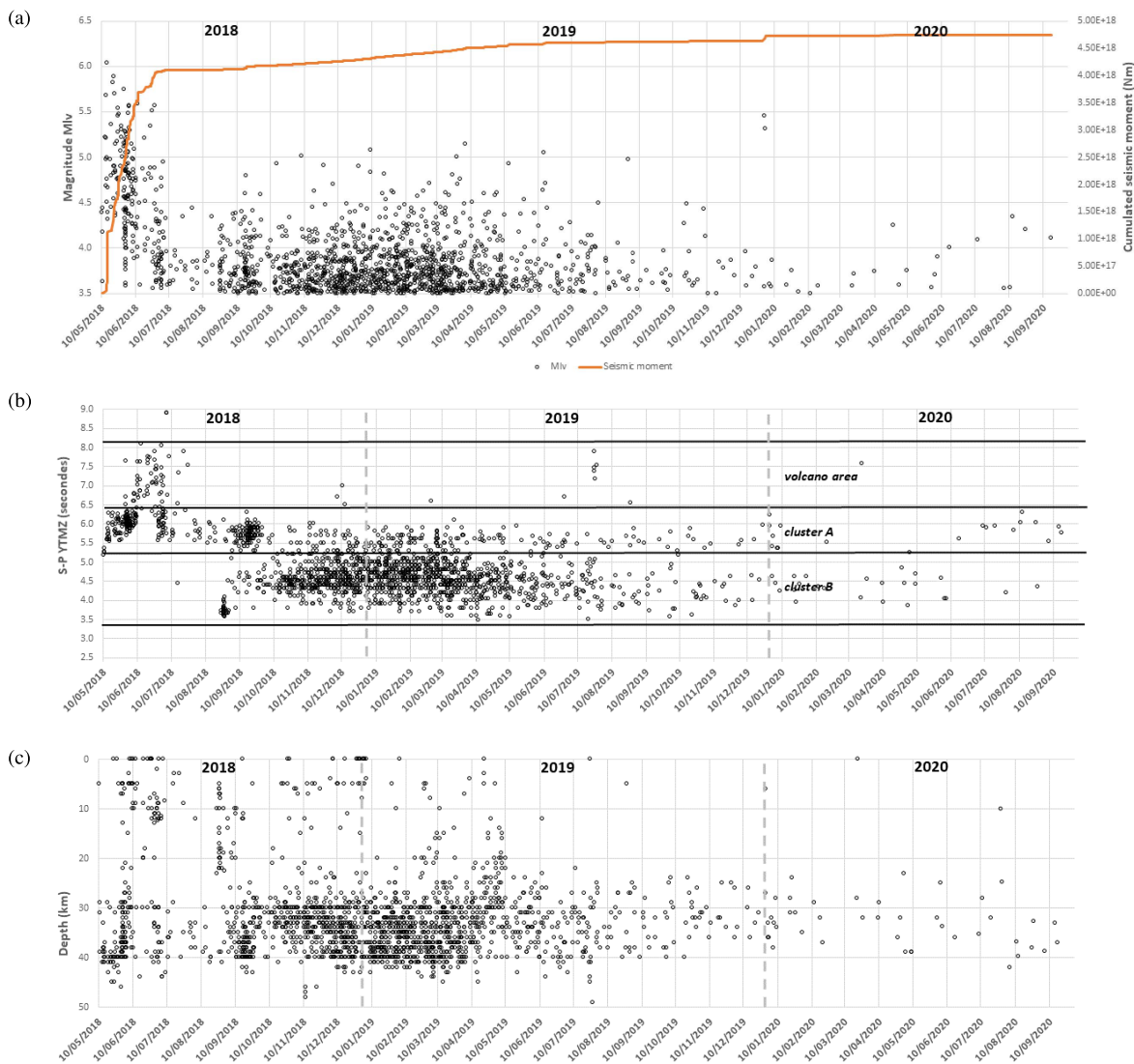


Figure 6. (a) Time evolution of magnitude for $M_{lv} > 3.5$ events for 2018–2020 Mayotte seismo-volcanic sequence (black dots) and cumulative seismic moment (orange line). (b) Evolution of S-P arrivals from station YTMZ with time with S-P limits for clusters A and B and the new volcanic edifice area. (c) Evolution of focal depth with time.

improvement of the monitoring network, not only for the survey of the current seismic sequence offshore of Mayotte, but also, for instance, for the survey of the regular volcanic activity in Karthala (OVK), the recent seismic datasets give an accuracy on the hypocentral parameters for the events affecting the whole archipelago that had not been reached up to now.

It is for the first time that all the seismicity data from the Comoros and its surroundings is gathered in

a comprehensive and homogeneous catalogue. Our new catalogue allows a better analysis of seismicity distribution and magnitudes. The seismicity appears mainly distributed along the Comoros archipelago, with earthquakes of magnitude higher than 5.0 occurring around the islands (Figure 2). Moreover, the epicentres are relatively aligned from east of Mayotte to the Leven bank following a $N70-90^\circ E$ oriented 100-km-wide band, while the seismicity is more

diffuse to the west of Mayotte, between Mayotte and Grande Comore. This distribution of seismicity could be either phenomenological, due to an area of more distributed deformation westward from west of Mayotte island or partly related to location biases due to the monitoring network limitations and its geometry before its recent improvement. Remarkably, even though the catalogue is incomplete until only recently, the recent Mayotte seismic sequence together with its large event of Mw 5.9 and the long-lasting swarms appear to be unique in the seismic history of the region. Located offshore, only marine surveys [e.g. Thinon *et al.*, 2020] may indicate if such ocean bottom volcanic eruptions and sequences occurred in the past. In any case it probably means that similar large seismo-volcanic sequences occur over centennial or millennial timescales, in accordance with the long-lasting Neogene volcanic activity in the Comoros islands and the slow strain in the region.

6.2. Hypocentre depth

The hypocentre depths of our catalogue remain poorly constrained, in particular for offshore events far from the seismic stations. A large number of regional earthquakes located by the ISC have a fixed depth of 10 km. For the eight earthquakes with GCMT locations in the Comoros region and outside of the recent Mayotte sequence, their depths range from 15 to 55 km. Better constraints on the focal depth of the main events of the area would be crucial for pointing out spatial variations of the seismogenic layer and eventually identifying distinct active regions.

From 2018, most earthquakes of the Mayotte sequence are between 20 and 45 km depth, i.e. below the Moho, whose depth is estimated around 20 km [Barruol *et al.*, 2018] (Figure 6c). The depths from the GCMT catalogue and from our catalogue are consistent and show a progressive rise of the hypocentres between 10 May and 27 June 2018: mean depth of 39 km, 25 km and 4 km respectively in May, the first half of June, and the second half of June [see Figure 6 from Lemoine *et al.*, 2020a, Cesca *et al.*, 2020, Supplementary Table S2].

For the period from 26 August 2018 to 1 October 2020, the comparison of mean depths between Cluster A (30 ± 13 km) and Cluster B (33 ± 6 km) does not show a significant difference. Locations using OBS from late February 2019 are clearly more suitable to

better estimate the focal depth for offshore events [Saurel *et al.*, 2021].

6.3. Focal mechanisms and seismotectonics

Between Mayotte and the Leven bank, the distribution of seismicity from our catalogue forms a N70–90° E 100-km-wide band. At large scale, this direction is reminiscent of the N81° E azimuth of one of the nodal planes of the largest event of the Mayotte seismic sequence (Mw 5.9 on 15 May 2018). Similar focal mechanisms were observed for most of the large events of the Mayotte seismo-volcanic sequence (Figure 3), but also to the east, like the event of 23 June 2007 recorded in Zelee & Geysers banks (Figure 2) and some of the events west of Mayotte (Figure 2). Although our catalogue is incomplete and the locations of small magnitude earthquakes disputable, these observations are consistent with an interpretation that considers the Comoros archipelago as an E–W striking right-lateral plate boundary [e.g., Kusky *et al.*, 2007, Stamps *et al.*, 2018]. At a more local scale, both field observations of tectonic (faults) and magmatic (dykes) structures in the Moheli, Anjouan and Mayotte islands are compatible with regional E–W right-lateral strike-slip shear [Famin *et al.*, 2020], as also the features of the Mayotte seismo-volcanic current phenomenon, which are consistent with transtensional behaviour in the area [Lemoine *et al.*, 2020a, Feuillet *et al.*, 2021].

West of Mayotte, the earthquake distribution does not underline a preferential direction. The lack of observed spatial organization of the seismicity could result either from a poor monitoring network as mentioned above or from more distributed deformation. Differences between the ISC and GCMT epicentral locations can reach more than 30 km for both the Mw = 5.2 Moheli 2000 and 2016 earthquakes and the Mw = 5.0 2011 event located between Anjouan and Mayotte. Together, epicentre location uncertainties, the large spread of seismicity, as well as a wider zone of deformation, also underlined by the north-south extension of the Grande Comore volcanic island for instance, make any simple interpretation of the seismicity west of Mayotte difficult. In addition, the few focal mechanisms (Figure 2) in the area show large variations. All together, the seismicity pattern revealed by our catalogue, underlines its limitation, but may also result from an immature plate

boundary making its way across an old oceanic lithosphere with a slow strain rate.

6.4. *Does the Mayotte seismic sequence improve the understanding of regional seismicity?*

Only eight earthquakes were recorded in the region of the Mayotte seismic sequence before 2018, all of them during the 1978–1995 period covered by the catalogue compiled by Bertil and Regnault [1998]. With a magnitude of $M_w = 4.8$ (or $m_b = 4.4$), the strongest event occurred on 01/03/1990 and was not detected by the international networks. For all the events in this area, no related swarm activity has been described and their small number and large location uncertainties prevent the detection of a specific direction from their spatial distribution.

With respect to the number of events and their magnitude, the recent sequence east of Mayotte is thus unprecedented. Although the Mayotte 2018–2020 swarm of epicentres is located in the already mentioned east–west band of events observed to the east of Mayotte as far as the Leven Bank, it occurs in an area without significant events before 2018. From recent bathymetric mapping east of Mayotte [Audru *et al.*, 2006, Paquet *et al.*, 2019, Feuillet *et al.*, 2021], a volcanic ridge between the island of Mayotte and the new volcano follows a $N110^\circ$ E trend. Both clusters A and B and the new volcanic edifice are broadly distributed along this alignment of submarine volcanic cones. However, the intense seismicity that preceded the onset of the eruption was associated with magmatic dyke propagation [Cesca *et al.*, 2020, Lemoine *et al.*, 2020a, Feuillet *et al.*, 2021]. Inversion of GNSS data covering the “magma ascent phase” constrained a $N138^\circ$ E-trending conduit [Lemoine *et al.*, 2020a] that would correspond to an opening in the $N48^\circ$ E direction. Although GCMT focal mechanisms reported at the beginning of the Mayotte seismic sequence show mostly strike-slip faulting with average and mean scatters of $260 \pm 12^\circ$, $85 \pm 11^\circ$ and $152 \pm 9^\circ$ for one plane, they are consistent with a NE–SW direction of extension. In other words, the seismicity that preceded the eruption and the events of Cluster A results from a large-scale magmatic process that interacted with the regional tectonic stress field.

Moreover, further north, the Jumelles volcanic ridges follow a $N135^\circ$ E orientation. Onshore, most

of the volcanic feeder dykes reported by Nehlig *et al.* [2013] northwest of Mayotte island show a mean azimuth of $N140^\circ$ E. Intense magmatic processes at the origin of this exceptional sequence are consistent with the regional context [focal mechanisms, dyke orientations, distribution of seismicity; Famin *et al.*, 2020, Lemoine *et al.*, 2020a, Feuillet *et al.*, 2021]. Within the framework of this sequence, a strong interaction between volcanism and tectonics can be observed, but their respective impact is yet to be understood.

6.5. *Does the seismicity of the Comoros Archipelago reveal the Lwandle–Somali plates boundary and its kinematics?*

The plate kinematic models deduced from regional geodetic studies in southeastern Africa and the southwestern Indian Ocean require the existence of the Lwandle plate between the Nubia and Rovuma plates to the west and the Somali plate to the east [Horner-Johnson *et al.*, 2007, Saria *et al.*, 2013, Stamps *et al.*, 2018]. The northern and eastern boundaries of this plate remain however poorly constrained. Some studies infer a boundary separating the Lwandle and Somali plates that would longitudinally cross central Madagascar [Horner-Johnson *et al.*, 2007, Saria *et al.*, 2013, Stamps *et al.*, 2014]. However, there is no evidence of east–west striking active faults across the island of Madagascar. Seismotectonic studies in Madagascar propose east–west extension associated with both the presence of localized graben and volcanic activity to the north and in the centre [Bertil and Regnault, 1998, Rindraharisaona *et al.*, 2013, Rakotondraibe *et al.*, 2020]. It has been proposed that the Lwandle northern plate boundary is located at the level of the Comoros archipelago [Kusky *et al.*, 2007, Stamps *et al.*, 2018, Famin *et al.*, 2020]. Geodetic data, although sparse, are in agreement with a right-lateral strike-slip boundary consistent with onshore fault kinematic indicators [Famin *et al.*, 2020], compatible with the presence of seismicity across the northern Mozambique Channel (Figure 2) and some of the large earthquake focal mechanisms (Figure 1). The large spread of seismicity across the Comoros archipelago as well as the seismicity gaps westward towards the Davie Ridge and eastward towards the coasts of Madagascar (Figures 1 and 2) have been

interpreted as the existence of either a diffuse plate boundary [e.g., Stamps *et al.*, 2020] or a segmented and immature volcano-tectonic strike-slip shear zone [e.g., Famin *et al.*, 2020, Feuillet *et al.*, 2021].

7. Conclusion and perspectives

Our catalogue is the first at this scale, integrating historical and instrumental seismicity of the Comoros archipelago. The lack of archives and data available for the area makes it difficult to compile such a catalogue. Although the region is moderately seismic, the Mayotte 2018–2020 seismic sequence underlines the importance of improving the knowledge of seismic hazard in the region and therefore of having a seismicity catalogue as exhaustive as possible.

The seismicity of the region highlights the activity of structures associated with the continuity of the East African Rift to the south, in particular the Kermimba Basin and the Davie Ridge, with mainly normal fault mechanisms.

On the island of Grande Comore, a large part of the seismicity is related to the Karthala volcano, suggesting that most of the activity is of volcano-tectonic origin. East of Grande Comore, the origin of the seismicity remains more ambiguous. The analysis of our catalogue suggests the existence of a deformation zone more distributed in the western part of the archipelago, whereas the seismicity seems more concentrated eastward from Mayotte. The rare focal mechanisms are consistent with a strike-slip stress regime.

At the regional scale, the seismo-volcanic sequence of 2018–2020 is exceptional and unexpected:

- due to the very long duration of the seismic-volcanic sequence (more than 2 years) and the maximum magnitude reached ($M_w = 5.9$),
- because of the complexity of the spatial distribution with two distinct clusters and the setting up of a volcano outside these two clusters,
- from the positioning of this volcanic swarm to the east of Mayotte, whereas the active volcano of the archipelago (Karthala) is 280 km away and the most recent volcanism of Mayotte was several thousands of years old.

In addition, the seismo-volcanic sequence is set up in the middle of a zone of moderate diffuse seismicity

several hundreds of kilometres wide, little known and not monitored until now. Neither is there any trace in the memory of the population nor in the historical archives, of an equivalent phenomenon with hundreds of earthquakes felt in a few months.

Seismic monitoring has been set up progressively without being able to surround the sequence zone because of the island context, until OBS deployments nine months after the unrest in the seismic sequence. It is only from March 2019 that three broadband stations were set up in Mayotte and one in Glorieuses as part of the scientific Tellus-Mayotte programme (CNRS/INSU). These stations are maintained till today as part of the monitoring mission of the Volcanological and Seismological Monitoring Network of Mayotte REVOSIMA set up in June 2019.

At the same time, MAYOBS oceanographic campaigns have allowed the monitoring of seismic and volcanic activity thanks to a network of OBS regularly deployed and recovered (DOI 10.18142/291). The processing of these data is done in collaboratively after each OBS recovery [Saurel *et al.*, 2021]. This treatment concerning only the strongest events, for all the records, detection methods and automatic localizations are currently developed [Retailleau *et al.*, 2020].

Research on seismicity data accumulated since 2018 has just begun. The locations of the first months of the crisis have been taken up again [Mercury *et al.*, 2020], refining the spatio-temporal evolution of the first months of the seismic sequence. The network installed in 2019 (ground onshore stations and offshore OBS) allows to analyse the structure of clusters [Jacques *et al.*, 2020], with an even finer vision by relative hypoDD localizations [Hoste-Colomer *et al.*, 2020]. The detection, localization and characterization of VLP events are the subject of specific studies in progress [Laurent *et al.*, 2020]. Volcanic plumbing system is analysed using local passive tomography [Foix and Aiken, 2020], petrological studies [e.g. Berthod *et al.*, 2021] or magnetotelluric sounding [Darnet *et al.*, 2020].

The volcano formation and evolution is described by Feuillet *et al.* [2021].

There are still knowledge gaps about the regional tectonic and geodynamic context. The ANR Coyotes project [<https://anr.fr/Projet-ANR-19-CE31-0018>, Thion *et al.*, 2020] aims to understand the

distribution of active and recent deformations around the Comoros archipelago, to visualize the crustal structuring and to study the recent tectono-sedimentary evolution. It is based on an oceanographic campaign SISMAORE [<http://www.geocean.net/coyotes/doku.php?id=autreprojet2:start>, Thinon *et al.*, 2020]. The still largely unknown oceanic bottom may reveal submarine structures that could explain the diffuse regional seismicity described here.

The REVOSIMA seismological monitoring network, with the stations installed in Mayotte and the sharing of regional data, has made it possible to lower very significantly the detection threshold at magnitude 2.5 to 3 around Mayotte and to 3.5 over the whole region.

We therefore expect rapid evolution of knowledge in the coming years in the hope of answering some of the current questions on the seismic behaviour in the area.

Acknowledgements

The monitoring of regional seismicity and the 2016–2020 Mayotte seismic swarm presented in our catalogue benefited from internal BRGM funding for the “Observatoire Sismologique” project. The relocation work is part of Nicolas Mercury’s thesis funded by BRGM, the French Ministry of Ecological Transition (DGPR) and CNRS/EOST/IPGS.

The seismic signals used in this study are from the following station networks: Geofon (doi:10.14470/TR560404), Iris/IDA (<https://doi.org/10.7914/SN/II>) Geoscope (doi:10.18715/GEOSCOPE.G), Observatoire du Karthala OVK (<http://www.cndrs-comores.org/observatoires/ovk/>), RESIF-RAP (doi:10.15778/RESIFRA).

The MCHI station was installed as part of the Sismo-à-l’école educational network (<http://edumed.unice.fr/fr>) with funding from BRGM, DEAL-Mayotte, Rectorat de Mayotte.

The Raspberry Shake stations were installed by EOST.

The broadband stations in Mayotte and on the island of Glorieuses were installed in 2019 as part of the Tellus-Mayotte programme (CNRS-INSU) in partnership with IGP/CNRS/BRGM/IFREMER/IPGS funded by “Ministère de l’Enseignement Supérieur de la Recherche et de l’Innovation” and by “Ministère de la Transition Ecologique et Solidaire”.

The maintenance of this network is done since 2020 within the framework of the Réseau de surveillance Volcanologique et Sismologique de Mayotte (REVOSIMA).

The authors would like to thank the anonymous reviewers for their comments, which helped to improve the article.

Supplementary data

Supporting information for this article is available on the journal’s website under <https://doi.org/10.5802/crgeos.79> or from the author.

References

- Adams, R. D., Hughes, A. A., and McGregor, D. M. (1982). Analysis procedures at the International Seismological Centre. *Phys. Earth Planet. Inter.*, 30, 85–93.
- Albaric, J., Perrot, J., Deverchère, J., Deschamps, A., Le Gall, B., Ferdinand, R. W., Petit, C., Tiberi, C., Sue, C., and Songo, M. (2010). Contrasted seismogenic and rheological behaviours from shallow and deep earthquake sequences in the North Tanzanian Divergence, East Africa. *J. Afr. Earth Sci.*, 58, 799–811.
- Ambraseys, N. N. and Adams, R. D. (1991). Reappraisal of major African earthquakes, south of 20° N, 1900–1930. *Nat. Hazards*, 4(4), 389–419.
- Audru, J. C., Guennoc, P., Thinon, I., and Abellard, O. (2006). Bathymay: la structure sous-marine de Mayotte révélée par l’imagerie multifaisceaux. *C. R. Geosci.*, 338(16), 1240–1249.
- Bachelery, P., Morin, J., Villeneuve, N., Soulé, H., Nasor, H., and Ali, A. R. (2016). Structure and eruptive history of Karthala volcano. In Bachelery, P., Lenat, J. E., Di Muro, A., and Michon, L., editors, *Active Volcanoes of the Southwest Indian Ocean. Active Volcanoes of the World*. Springer, Berlin, Heidelberg.
- Barruol, G., Dofal, A., Fontaine, F. R., Michon, L., and Tkalcic, H. (2018). Crustal structure variation across the southwestern Indian Ocean from receiver functions determined at Ocean-Bottom Seismometers. In *Abstract T43G-0497, 2018 Fall Meeting*. AGU, San Francisco. Bibcode: 2018AGUFM.T43G0497B.
- Barth, A., Wenzel, F., and Giardini, D. (2007). Frequency sensitive moment tensor inversion for light

- to moderate magnitude earthquakes in eastern Africa. *Geophys. Res. Lett.*, 34, 1–5.
- Bath, M. (1975). Seismicity of the Tanzania region. *Tectonophysics*, 27(4), 353–379.
- Berthod, C., Médard, E., Bachèlery, P., Gurioli, L., Di Muro, A., Peltier, A., Komorowski, J. C., Benbakkar, M., Devidal, J. L., Langlade, J., Besson, P., Boudon, G., Rose-Koga, E., Deplus, C., Le Friant, A., Bickert, M., Nowak, S., Thinon, I., Burckel, P., Hidalgo, S., Kaliwoda, M., Jorry, S., Fouquet, Y., and Feuillet, N. (2021). The 2018-ongoing Mayotte submarine eruption: magma migration imaged by petrological monitoring. *Earth Planet. Sci. Lett.*, 571, article no. 117085.
- Bertil, D. and Regnault, J. M. (1998). Seismotectonics of Madagascar. *Tectonophysics*, 294, 57–74.
- Bertil, D., Roullé, A., Lemoine, A., Colombain, A., Hoste-Colomer, R., Meza-Fajardo, K., Maisonhaute, E., and Dectot, G. (2019). MAYEQSwarm2019: BRGM earthquake catalogue for the Earthquake Swarm located East of Mayotte. 2018 May 10th–2019 May 15th, <https://doi.org/10.18144/rmg1-ts50>.
- Bondár, I. and Storchak, D. A. (2011). Improved location procedures at the International Seismological Centre. *Geophys. J. Int.*, 186, 1220–1244.
- Boulanger, J. (1953). Les tremblements de terre de Janvier-Février 1953 à la Grande Comore. Documentation du Bureau Géologique. No 70. Direction des Mines et de la Géologie. Haut Commissariat de Madagascar et Dépendances. 20 pp.
- Briole, P. (2018). Note sur la crise tellurique en cours à Mayotte. 26 Novembre 2018. http://volcano.iterre.fr/wp-content/uploads/2018/11/mayotte_note_deformation_GPS_20181126.pdf.
- Calais, E., d'Oreye, N., Albaric, J., and Deschamps, A. (2008). Strain accommodation by slow slip and dyking in a youthful continental rift, East Africa. *Nature*, 456, 783–787.
- Cesca, S. et al. (2020). Drainage of a deep magma reservoir near Mayotte inferred from seismicity and deformation. *Nat. Geosci.*, 13(1), 87–93.
- Cesca, S., Letort, J., Razafindrakoto, H. N. T., Heimann, S., Rivalta, E., Isken, M., Passarelli, L., Nikkhoo, M., Petersen, G. M., Cotton, F., and Dahm, T. (2019). The 2018–2019 seismo-volcanic crisis offshore Mayotte: depletion of a deep offshore magmatic reservoir. In *Abstract #V52D-04, 2019 Fall Meeting*. AGU, San Francisco.
- Chorowicz, J. (2005). The East African rift system. *J. Afric. Earth Sci.*, 43, 79–410.
- Coffin, M. F. and Rabinowitz, P. D. (1987). Reconstruction of Madagascar and Africa: evidence from the Davie fracture zone and western Somali basin. *J. Geophys. Res.*, 92(B9), 9385–9406.
- Courgeon, S., Bachèlery, P., Jouet, G., Jorry, S. J., Bou, E., BouDagher-Fadel, M. K., Révillon, S., Camoin, G., and Poli, E. (2018). The offshore east African rift system: new insights from the Sakalaves seamounts (Davie Ridge, SW Indian Ocean). *Terra Nova.*, 30(5), 380–388.
- Craig, T. J., Jackson, J. A., Priestly, K., and McKenzie, D. (2011). Earthquake distribution patterns in Africa: Their relationship to variations in lithospheric and geologic structure, and their rheological implications. *Geophys. J. Int.*, 185, 403–434.
- Cucciniello, C., Melluso, L., Morra, V., Storey, M., Rocco, I., Franciosi, L., Grifa, C., Petrone, C. M., and Vincent, M. (2011). New ^{40}Ar – ^{39}Ar ages and petrogenesis of the Massif d'Ambre volcano, northern Madagascar. In *Geological Society of America Special Papers*, volume 478, pages 257–281.
- Darnet, M., Wawrzyniak, P., Tarits, P., Hautot, S., and D'Eu, J. F. (2020). Mapping the geometry of volcanic systems with magnetotelluric soundings: Results from a land and marine magnetotelluric survey performed during the 2018–2019 Mayotte seismovolcanic crisis. *J. Volcanol. Geotherm.*, 406, article no. 107046.
- Davis, J. K., Lawver, L. A., Norton, I. O., and Gahagan, L. M. (2016). New Somali basin magnetic anomalies and a plate Model for the early Indian ocean. *Gondwana Res.*, 34, 16–28.
- Deplus, C., Feuillet, N., Bachelery, P., Fouquet, Y., Jorry, S., Thinon, I., Bermell, S., Besson, F., Gaillot, A., Guérin, C., Le Friant, A., Paquet, F., Pierre, D., and Pitel-Roudaut, M. (2019). Early development and growth of a deep seafloor volcano: Preliminary results from the MAYOBS cruises. In *Abstract V43I-0227, 2019 Fall Meeting*. AGU, San Francisco.
- Déprez, A., Doubre, C., Masson, F., and Ulrich, P. (2013). Seismic and aseismic deformation along the East African rift system from a reanalysis of the GPS velocity field of Africa. *Geophys. J. Int.*, 193, 1353–1369.
- Deville, E., Marsset, T., Courgeon, S., Jatiault, R., Ponte, J., Thereau, E., Jouet, G., Jorry, S. J., and Droz, L. (2018). Active fault system across the oceanic

- lithosphere of the Mozambique Channel: Implications for the Nubia – Somalia southern plate boundary. *Earth Planet. Sci. Lett.*, 502, 210–220.
- Di Giacomo, D., Bondár, I., Storchak, D. A., Engdahl, E. R., Bormann, P., and Harris, J. (2015a). ISC-GEM: Global instrumental earthquake catalogue (1900–2009): III. Re-computed MS and mb, proxy MW, final magnitude composition and completeness assessment. *Phys. Earth Planet. Int.*, 239, 33–47.
- Di Giacomo, D., Engdahl, E. R., and Storchak, D. A. (2018). The ISC-GEM earthquake catalogue (1904–2014): status after the Extension Project. *Earth Syst. Sci. Data*, 10, 1877–1899.
- Di Giacomo, D., Harris, J., Villaseñor, A., Storchak, D. A., Engdahl, E. R., Lee, W. H. K., and the Data Entry Team (2015b). ISC-GEM: Global instrumental earthquake catalogue (1900–2009), I. Data collection from early instrumental seismological bulletins. *Phys. Earth Planet. Int.*, 239, 14–24.
- Dziewonski, A. M., Chou, T. A., and Woodhouse, J. H. (1981). Determination of earthquake source parameters from waveform data for studies of global and regional seismicity. *J. Geophys. Res.*, 86, 2825–2852.
- Ekström, G., Nettles, M., and Dziewoński, A. (2012). The global CMT project 2004–2010: Centroid-moment tensors for 13,017 earthquakes. *Phys. Earth Planet. Inter.*, 200, 1–9.
- Famin, V., Michon, L., and Bourhane, A. (2020). The Comoros archipelago: A right-lateral transform boundary between the Somalia and Lwandle plates. *Tectonophysics*, 789, article no. 228539.
- Feuillet, N., Jorry, S., Crawford, W., Deplus, C., Thignon, I., Jacques, E., Saurel, J. M., Lemoine, A., Paquet, F., Satriano, C., Aiken, C., Foix, O., Kowalski, P., Laurent, A., Rinnert, E., Cathalot, C., Donval, J. P., Guyader, V., Gaillot, A., Scalabrin, C., Moreira, M., Peltier, A., Beauducel, F., Grandin, R., Ballu, V., Daniel, R., Pelleau, P., Besançon, S., Geli, L., Bernard, P., Bachelery, P., Fouquet, Y., Bertil, D., Lemarchand, A., and Van der Woerd, J. (2021). Birth of a large volcano offshore Mayotte through lithosphere-scale rifting. *Nat. Geosci.* (accepted), <https://doi.org/10.1038/s41561-021-00809-x>.
- Feuillet, N., Jorry, S., Crawford, W. C., Deplus, C., Thignon, I., Jacques, E., Saurel, J. M., Lemoine, A., Paquet, F., Daniel, R., Gaillot, A., Satriano, C., Peltier, A., Aiken, C., Foix, O., Kowalski, P., Laurent, A., Beauducel, F., Grandin, R., Ballu, V., Bernard, P., Donval, J. P., Géli, L., Gomez, J., Pelleau, P., Guyader, V., Rinnert, E., Besançon, S., Bertil, D., Lemarchand, A., Van der Woerd, J., et al. (2019a). Birth of a large volcano offshore Mayotte through lithosphere-scale rifting. In *Abstract V52D-01, 2019 Fall Meeting*. AGU, San Francisco.
- Feuillet, N., Jorry, S., Rinnert, E., Thignon, I., and Fouquet, Y. (2019b). MAYOBS. <https://doi.org/10.18142/291>.
- Flower, M. F. J. and Strong, D. F. (1969). The significance of sandstone inclusions in lavas of the Comores Archipelago. *Earth Planet. Sci. Lett.*, 7(1), 47–50.
- Foix, O. and Aiken, C. (2020). Offshore Mayotte Volcanic plumbing revealed by local passive tomography. In *Fall Meeting 2020, Abstract #V043-02*. American Geophysical Union, USA.
- Foster, A. N. and Jackson, J. A. (1998). Source parameters of large African earthquakes: implications for crustal rheology and regional kinematics. *Geophys. J. Int.*, 1998(2), 422–448.
- Franke, D., Jokat, W., Ladage, S., Stollhofen, H., Klimke, J., Lutz, R., Mahanjane, E. S., Ehrhardt, A., and Schreckenberger, B. (2015). The offshore East African Rift System: Structural framework at the toe of a juvenile rift. *Tectonics*, 34, 2086–2104.
- Gevrey, A. (1870). *Essai sur les Iles Comores*. A. Saligny (Pondichery). <ark:/12148/bpt6k62208586>.
- Grimison, N. L. and Chen, W. P. (1988). Earthquakes in the Davie Ridge–Madagascar region and the southern Nubian–Somalian plate boundary. *Geophys. Res.*, 93, 10439–10450.
- Gutenberg, B. and Richter, C. (1954). *Seismicity of the Earth and Associated Phenomena*. Princeton University Press, Princeton, NJ.
- Hachim, S. (2004). Catastrophes: Mayotte perd sa mémoire! Catastrophes naturelles et mémoire collective à Mayotte. Mémoire de DEA de Géographie, Université Paul Valéry, Montpellier III.
- Hartnady, C. J. H. (2002). Earthquake hazard in Africa: perspectives on the Nubia-Somalia boundary. *South African J. Sci.*, 98(9), 425–428.
- Horner-Johnson, B. C., Argus, D. F., and Gordon, R. G. (2007). Plate kinematic evidence for the existence of a distinct plate between the Nubian and Somalian plates along the Southwest Indian Ridge. *J. Geophys. Res.*, 112, article no. B05418.
- Hoste-Colomer, R., Jacques, E., Lemoine, A., Lavayssière, A., Crawford, W. C., Feuillet, N.,

- Fouquet, Y., Jorry, S., Rinnert, E., Thinon, I., and MAYOBS/REVOSIMA Seismology group (2020). 2019 Seismicity clusters structure of Mayotte volcano-tectonic crisis. In *Fall Meeting 2020, Abstract #V040-0001*. American Geophysical Union, USA.
- International Seismological Centre (2021). On-line Bulletin. <https://doi.org/10.31905/D808B830>.
- Jacques, E., Feuillet, N., Aiken, C., Lemoine, A., Crawford, W. C., Deplus, C., Thinon, I., Saurel, J. M., Bès de Berc, M., Broucke, C., Colombain, A., Daniel, R., Dectot, G., Dofal, A., Foix, O., Gomez, J., Grunberg, M., Kowalski, P., Laurent, A., Léger, F., Lemarchand, A., and Pelleau, P. (2019). The 2018–2019 Mayotte seismic crisis: Evidence of an upper mantle rifting event? In *Abstract V43I-0221, 2019 Fall Meeting*. AGU, San Francisco. Bibcode: 2019AGUFM.V43I0221J.
- Jacques, E., Hoste-Colomer, R., Lavayssière, A., Lemoine, A., Crawford, W. C., Feuillet, N., Fouquet, Y., Jorry, S., Rinnert, E., Thinon, I., Van der Woerd, J., and MAYOBS/REVOSIMA Seismology group (2020). Seismo-tectonic analysis of the ongoing Mayotte crisis suggesting reactivation of a caldera structure below the Moho. In *Fall Meeting 2020, Abstract #V040-0006*. American Geophysical Union, USA.
- König, M. and Jokat, W. (2010). Advanced insights into magmatism and volcanism of the Mozambique Ridge and Mozambique Basin in the view of new potential field data. *Geophys. J. Int.*, 180(1), 158–180.
- Kusky, T. M., Toraman, E., and Raharimahefa, T. (2007). The great rift valley of Madagascar: An extension of the Africa-Somali plate boundary? *Gondwana Res.*, 11, 577–579.
- Kusky, T. M., Toraman, E., Raharimahefa, T., and Rasozanamparany, C. (2010). Active tectonics of the Alaotra–Ankay Graben System, Madagascar: possible extension of Somalian–African diffusive plate boundary? *Gondwana Res.*, 18(2–3), 274–294.
- Lacroix, A. (1920). Une éruption du volcan Karthala à la Grande Comore en août 1918. *C. R. Acad. Sci. Paris*, 171, 5–10.
- Lambert, J. (1997). Contribution au relevé de la sismicité historique des îles de la Réunion, de Maurice et des Comores. BRGM R39736, 56 p.
- Laurent, A., Satriano, C., Bernard, P., Feuillet, N., and Jorry, S. (2020). Detection, location and characterization of VLF events during the 2018–2020 seismo-volcanic crisis in Mayotte. In *Fall Meeting 2020, Abstract #V040-0004*. American Geophysical Union, USA.
- Lavayssière, A., Crawford, W. C., Saurel, J. M., and Satriano, C. (2020). New 1D velocity model and absolute locations image Mayotte seismo-volcanic region. In *Fall Meeting 2020, Abstract #V040-0005*. American Geophysical Union, USA.
- Laville, E., Piqué, A., Plaziat, J.-C., Gioan, P., Rakotomalala, R., Ravololonirina, Y., and Tidahy, E. (1998). Le fossé méridien d'Ankay-Alaotra, témoin d'une extension crustale récente et actuelle à Madagascar. *Bull. Soc. Géol. France*, 169(6), 775–788.
- Le Gall, B. et al. (2004). Neogene-recent rift propagation in central Tanzania: morphostructural and aeromagnetic evidence from the Kilombero area. *Geol. Soc. Am. Bull.*, 116, 490–510.
- Lee, W. H. K. and Valdes, C. M. (1985). In *HYPO71PC: A Personal Computer Version of the HYPO71 Earthquake Location Program*, volume 85, No. 749. US Geological Survey.
- Lemoine, A., Bertil, D., Roullé, A., Briole, P., Foumelis, M., Saurel, J. M., Jacques, E., Aiken, C., Colombain, A., Hoste-Colomer, R., Thinon, I., Raucoules, D., de Michele, M., Lemarchand, A., and Dectot, G. (2019). The 2018–2019 seismo-volcanic crisis east of Mayotte, Comoros islands: first months of seismicity and deformation observations. In *Abstract V52D-02, 2019 Fall Meeting*. AGU, San Francisco. Bibcode: 2019AGUFM.V52D.02L.
- Lemoine, A., Briole, P., Bertil, D., Roullé, A., Foumelis, M., Thinon, I., Raucoules, D., de Michele, M., Valty, P., and Colomer, R. H. (2020a). The 2018–2019 seismo-volcanic crisis east of Mayotte, Comoros Islands: Seismicity and ground deformation markers of an exceptional submarine eruption. *Geophys. J. Int.*, 223, 22–44.
- Lemoine, A., Pedreros, R., and Filippini, A. (2020b). Scénarios d'impact des tsunamis pour Mayotte. Technical Report BRGM/RP-69869-FR. 169 p., 21 ill., 8 Tab., 61 ann.
- Leroux, E., Counts, J. W., Jorry, S. J., Jouet, G., Révillon, S., BouDagher-Fadel, M. K., Courgeon, S., Berthod, C., Ruffet, G., Bachèlery, P., and Grenard-Grand, E. (2020). Evolution of the Glorieuses seamount in the SW Indian Ocean and surrounding deep Somali Basin since the Cretaceous. *Mar. Geol.*, 427, article

- no. 106202.
- Malod, J. A., Mougénot, D., Raillard, S., and Maillard, A. (1991). Nouvelles contraintes sur la cinématique de Madagascar: les structures de la chaîne de Davie. *C. R. Acad. Sci. Paris*, 312(II), 1639–1646.
- Mercury, N., Lemoine, A., Bertil, D., Van der Woerd, J., Doubre, C., and Hoste-Colomer, R. (2020). The 2018–2020 seismo-volcanic crisis, east of Mayotte, Comoros islands: in-depth study of poorly instrumented first months of crisis. In *Fall Meeting 2020, Abstract #V040-0007*. American Geophysical Union, USA.
- Michon, L. (2016). The volcanism of the Comores archipelago integrated at a regional scale. In Bachèlery, P., Lénat, J.-F., Di Muro, A., and Michon, L., editors, *Active Volcanoes of the Southwest Indian Ocean: Piton de La Fournaise and Karthala*, pages 333–344. Springer-Verlag, Berlin and Heidelberg.
- Morgan, W. J. (1972). Deep mantle convection plumes and plate motions. *AAPG Bull.*, 56(2), 203–213.
- Mougénot, D., Recq, P., Virlogeux, P., and Lepvrier, C. (1986). Seaward extension of East Africa rift. *Nature*, 321, 1639–1646.
- Nehlig, P., Lacquement, F., Bernard, J., Caroff, M., Deparis, J., Jaouen, T., Pelleter, A., Perrin, J., Prognon, C., and Vittecoq, B. (2013). Notice de la carte géologique de Mayotte. Technical Report BRGM/RP-61803-FR. 143 pp, 45 fig., 1 ann.
- Noble, W. P., Foster, D. A., and Gleadow, A. J. W. (1997). The post-Pan-African thermal and extensional history of crystalline basement rocks in eastern Tanzania. *Tectonophysics*, 275(4), 331–350.
- Paquet, F., Jorry, S., Deplus, C., Le Friant, A., Bernard, J., Bremell-Fleury, S., and Thinon, I. (2019). The Mayotte Seismo-volcanic crisis: Characterizing a reactivated volcanic ridge from the upper slope to the Abyssal plain using multibeam bathymetry and backscatter data. In *Abstract #V43I-0219, 2019 Fall Meeting*. AGU, San Francisco. Bibcode: 2019AGUFM.V43I0219P.
- Pelleter, A. A., Caroff, M., Cordier, C., Bachelery, P., Nehlig, P., Debeuf, D., and Arnaud, N. (2014). Melilite-bearing lavas in Mayotte (France): An insight into the mantle source below the Comores. *Lithos*, 208–209, 281–297.
- Phethean, J. J. J., Kalnins, L. M., van Hunen, J., Biffi, P. G., Davies, R. J., and McCaffrey, K. J. W. (2016). Madagascar's escape from Africa: A high-resolution plate reconstruction for the Western Somali Basin and implications for supercontinent dispersal. *Geochem. Geophys. Geosyst.*, 17(12), 5036–5055.
- Poli, P., Nikolai, S., and Campillo, M. (2019). Teleseismic detection of very long period signals from Mayotte volcanic crisis. In *Abstract #V52D-08, 2019 Fall Meeting*. AGU, San Francisco. Bibcode: 2019AGUFM.V52D..08P.
- Rabinowitz, P. D., Coffin, M. E., and Falvey, D. (1983). The separation of Madagascar and Africa. *Science*, 220(4592), 67–69.
- Rakotondraibe, T., Nyblade, A. A., Wyssession, M. E., Durrheim, R. J., Rambolamanana, G., Aleqabi, G. I., Shore, P. J., Pratt, M. J., Andriampemanana, F., Rumpker, G., and Rindraharisaona, E. (2020). Seismicity and seismotectonics of Madagascar revealed by the 2011–2013 deployment of the island-wide MACOMO broadband seismic array. *Tectonophysics*, 790, article no. 228547.
- Rakotondrainibe (1977). *Contribution à l'étude de la sismicité de Madagascar*. PhD thesis, Faculté des sciences, Université d'Antananarivo.
- RESIF (1995). RESIF-RAP French Accelerometric Network. RESIF – Réseau Sismologique et géodésique Français. <http://dx.doi.org/10.15778/resif.ra>.
- Retailleau, L., Saurel, J. M., Issartel, S., Zhu, W., Beroza, G. C., Satriano, C., Ferrazzini, V., and Komorowski, J. C. (2020). Automatic detection of the seismicity associated to the Mayotte volcanic crisis. In *AGU Fall Meeting 2020 Online, December 2020*. AGU, USA.
- Rindraharisaona, E. J., Guidarelli, M., Aoudia, A., and Rambolamanana, G. (2013). Earth structure and instrumental seismicity of Madagascar: implications on the seismotectonics. *Tectonophysics*, 594, 165–181.
- Rufer, D., Preusser, F., Schreurs, G., Gnos, E., and Berger, A. (2014). Late Quaternary history of Vakinankaratra volcanic field (central Madagascar): insights from luminescence dating of phreatomagmatic eruption deposits. *Bull. Volcanol.*, 76, article no. 817.
- Saria, E., Calais, E., Altamimi, Z., Willis, P., and Farah, H. (2013). A new velocity field for Africa from combined GPS and DORIS space geodetic Solutions: Contribution to the definition of the African reference frame (AFREF). *J. Geophys. Res. Solid Earth*, 118(4), 1677–1697.

- Satriano, C., Laurent, A., Bernard, P., Grandin, R., Saurel, J. M., Lemarchand, A., Daniel, R., Jorry, S., Crawford, W. C., and Feuillet, N. (2019). Source process of the very low frequency earthquakes during Mayotte 2018–2019 Seismo-volcanic crisis. In *Abstract #V43I-0222, 2019 Fall Meeting. AGU, San Francisco*. Bibcode: 2019AGUFM.V43I0222S.
- Saurel, J. M., Aiken, C., Jacques, E., Lemoine, A., Crawford, W. C., Lemarchand, A., Daniel, R., Pelleau, P., Bès de Berc, M., Dectot, G., Bertil, D., Roullé, A., Broucke, C., Colombain, A., Besançon, S., Guyvarch, P., Kowalski, P., Roudaut, M., Dofal, A., Foix, O., Géli, L., Gomez, J., Grunberg, M., Laurent, A., Léger, E., Satriano, C., Tronel, F., Van der Woerd, J., Jorry, S., Thion, I., and Feuillet, N. (2019). High-resolution onboard manual locations of Mayotte seismicity since March 2019, using local land and seafloor stations. In *Abstract #V43I-0220, 2019 Fall Meeting. AGU, San Francisco*. Bibcode: 2019AGUFM.V43I0220S.
- Saurel, J. M., Jacques, E., Aiken, C., Lemoine, A., Retailleau, L., Lavyssiere, A., Foix, A., Dofal, A., Laurent, A., Mercury, N., Crawford, W., Lemarchand, A., Daniel, R., Pelleau, P., Bes de Berc, M., Dectot, G., Bertil, D., Roullé, A., Broucker, C., Colombain, A., Besancon, S., Guyavarch, P., Kowalski, P., Roudaut, M., Battaglia, J., Bodihar, S., Bouin, M. P., Canjamaile, K., Desfete, N., Doubre, C., Dretzen, R., Ferrazzini, V., Fontaine, F., Geli, L., Griot, C., Grunberg, M., Can Guzel, E., Hoste-Colomer, R., Lambotte, S., Leger, F., Vergnes, J., Satriano, C., Tronel, F., Vanderwoerd, J., Feuillet, N., Fouquet, Y., Jorry, S. J., Rinnert, E., and Thion, I. (2021). Mayotte seismic crisis: building knowledge in near real-time by combining land and ocean-bottom seismometers, first results. *Geophys. J. Int.* submitted.
- Savin, C., Grasso, J. R., and Bachelery, P. (2005). Seismic signature of a phreatic explosion: hydrofracturing damage at Karthala volcano, Grande Comore Island, Indian Ocean. *Bull. Volcanol.*, 67, 717–731.
- Scordilis, E. M. (2006). Empirical global relations converting MS and mb to moment magnitude. *J. Seismol.*, 10(2), 225–236.
- SISFRANCE-Océan Indien (2010). BRGM. https://sisfrance.irsn.fr/Reunion/index*.
- Snoke, J. A. (2003). FOCMEC: FOCal MECHANism determinations. In Lee, W. H. K., Kanamori, H., Jennings, P. C., and Kisslinger, C., editors, *International Hand-book of Earthquake and Engineering Seismology*, pages 1629–1630. Academic Press, San Diego. (Part B).
- Stamps, D. S., Flesch, L. M., Calais, E., and Ghosh, A. (2014). Current kinematics and dynamics of Africa and the East African Rift System. *J. Geophys. Res.*, 119, 5161–5186.
- Stamps, D. S., Kreemer, C., Fernandes, R., Rajaonarison, T. A., and Rambolamanana, G. (2020). Redefining East African Rift System kinematics. *Geology*, 49(2), 150–155.
- Stamps, D. S., Saria, E., and Kreemer, C. (2018). Geodetic strain rate model for the East African Rift System. *Sci. Rep.*, 8(1), article no. 732.
- Storchak, D. A., Di Giacomo, D., Bondár, I., Engdahl, E. R., Harris, J., Lee, W. H. K., Villaseñor, A., and Bormann, P. (2013). Public release of the ISC-GEM global instrumental earthquake catalogue (1900–2009). *Seism. Res. Lett.*, 84(5), 810–815.
- Sykes, L. R. and Landisman, M. (1964). The seismicity of east Africa, the Gulf of Aden and the Arabian and Red Seas. *Bull. Seismol. Soc. Am.*, 54(6A), 1927–1940. The Seismological Society of America.
- Thion, I., Lemoine, A., Feuillet, N., Michon, L., Leroy, S., et al. (2020). ANR COYOTES project (Comoros & maYotte: vOlcanism, TEctonics and Seismicity). In *Fall Meeting 2020, Abstract #V040-0003*. American Geophysical Union, USA.
- Tiberi, C., Gautier, S., Ebinger, C., Roecker, S., Plasman, M., Albaric, J., Déverchère, J., Peyrat, S., Perrot, J., Ferdinand Wambura, R., Msabi, M., Muzuka, A., Mulibo, G., and Kianji, G. (2019). Lithospheric modification by extension and magmatism at the craton-orogenic boundary: North Tanzania Divergence, East Africa. *Geophys. J. Int.*, 216(3), 1693–1710.
- Tzevahirtzian, A., Zaragosi, S., Bachèlery, P., Biscara, L., and Marchès, E. (2021). Submarine morphology of the Comoros volcanic archipelago. *Mar. Geol.*, 432, article no. 106383.
- Vienne, E. (1900). Notice sur Mayotte et les Comores. Impr Alcan-Lévy. 200 p. ark:/12148/bpt6k57903288.